This paper is published as part of a *Dalton Transactions* themed issue on:

Metal-catalysed Polymerisation

Guest Editors: Barbara Milani and Carmen Claver
University of Trieste, Italy and Universitat Rovira i Virgili, Tarragona, Spain

Published in issue 41, 2009 of *Dalton Transactions*

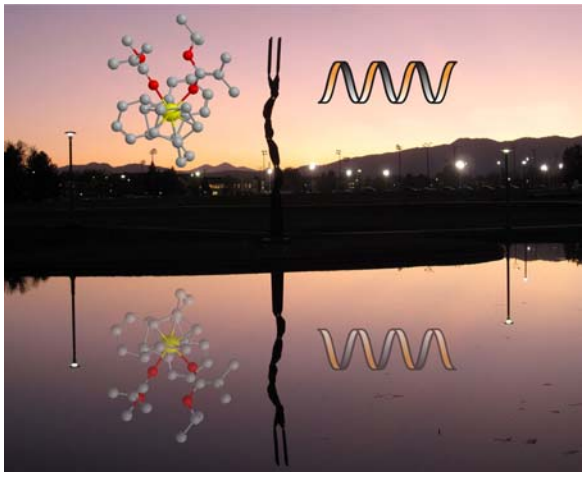

Image reproduced with permission of Eugene Chen

Articles published in this issue include:

PERSPECTIVES:

HOT PAPERS:

Visit the *Dalton Transactions* website for more cutting-edge organometallic and catalysis research
www.rsc.org/dalton

Palladium(II)-catalyzed copolymerization of styrenes with carbon monoxide: mechanism of chain propagation and chain transfer†

Francis C. Rix,[a] Michael J. Rachita,[a] Mark I. Wagner,[a] Maurice Brookhart,*[a] Barbara Milani[b] and James C. Barborak[c]

Received 11th June 2009, Accepted 7th August 2009
First published as an Advance Article on the web 3rd September 2009
DOI: 10.1039/b911392d

A mechanistic interpretation of the [(1,10-phenanthroline)Pd(CH_3)(CH_3CN)]$^+$[BArF]$^-$ (**1a**) and [(2,2′-bipyridine)Pd(CH_3)(CH_3CN)]$^+$[BArF]$^-$ (**1b**) (BArF = 3,5-$(CF_3)_2$-C_6H_3) catalyzed perfectly alternating copolymerization of styrenes with CO is reported. The copolymerization in CH_2Cl_2 or chlorobenzene has been found to be first order in styrene and inverse first order in CO concentrations. The microscopic steps involved in the catalytic cycle have been studied *via* low temperature NMR techniques. Palladium alkyl chelate complex [(2,2′-bipyridine)Pd(CHArCH$_2$C(O)CH$_3$)]$^+$[BArF]$^-$ (**5bσ**) and [(2,2′-bipyridine)Pd(η^3-CH(CH$_2$C(O)CH$_3$)Ar)]$^+$[BArF]$^-$ (**5bπ**), existing in equilibrium, were prepared. Treatment of **5σ,π** with ^{13}CO followed by 4-*tert*-butylstyrene at −78 °C allowed for ^{13}C NMR monitoring of the alternating chain growth of a series of palladium acyl carbonyl complexes. The acyl carbonyl species, representing the catalyst resting state, is in equilibrium with a palladium acyl styrene complex. The equilibrium constant, K_4, measured between [(phen)Pd(CO)(C(O)CH_3)]$^+$[BArF]$^-$ (**3a**) and [(phen)Pd(C(O)CH_3)-(C_6H_5C=CH_2)]$^+$[BArF]$^-$ (**8a**), was determined to be $2.84 \pm 2.8 \times 10^{-7}$ at −66 °C. The barrier to migratory insertion in **8a** was determined ($\Delta G^{\ddagger}$ (−66 °C) = 15.6 ± 0.1 kcal mol^{-1}). From the experimentally determined kinetic and thermodynamic data for the copolymerization of styrene with CO a mechanistic model has been constructed. The ability of this model to predict catalyst turnover frequency (TOF) was used as a test of its validity. A series of *para*-substituted styrenes, *p*-XC_6H_4CH=CH_2 (X = –OCH_3, –CH_3, –H, –Cl), were copolymerized with CO. A Hammett treatment of TOF for the series showed that electron-donating groups increase the rate of copolymerization ($\rho^p = -0.8$). The ratio of chain transfer to chain propagation was found to increase with styrene concentration and decrease with CO concentration. Polymer end group analysis showed the presence of α, β-enone end groups. The reactivity of model systems, coupled with a study of the effect of added acetonitrile, support a chain transfer mechanism involving β-hydrogen transfer to monomer from a palladium alkyl styrene intermediate.

Introduction

During the last fifteen years considerable interest has been focused on the synthesis of perfectly alternating carbon monoxide/alkene polyketones (eqn (1)). This reaction is homogeneously catalyzed by Pd(II) complexes containing a wide array of bidentate ligands including bidentate phosphine donors, bidentate nitrogen donors, hybrid phosphorus-nitrogen systems and phosphino-phosphite ligands.[1–9] A range of reaction conditions have been employed: CO pressures ranging from 1 to 40 bar, temperatures from 30 to 90 °C, and solvent variations including alcohols, dichloromethane, chlorobenzene and water. The addition of co-reagents, such as 1,4-benzoquinone (BQ), or co-catalysts, such as Brønsted acids is often advantageous. The choice of the best reaction conditions depends both on the nature of the palladium complex as pre-catalyst and on the nature of the alkene comonomer.

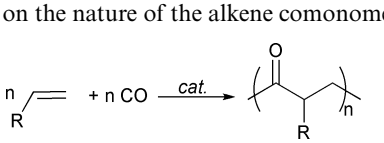

(1)

It is well known that diphosphine ligands are the ligands of choice when aliphatic alkenes are the comonomers; the *o*-anisole modified 1,3-bis(diphenyl phosphino) propane (bdompp) was applied for the industrial production of Carilon®, the CO/ethylene/propylene terpolymer.[10] Even though CO/vinyl arene co- and terpolymers were not exploited at a commercial level, the corresponding copolymerization reaction has been the subject of extensive investigations mainly aimed at understanding the factors affecting catalyst stability, polymer molecular weight[11–13] and polymer stereochemistry.[14–25] In addition, it was demonstrated that the nature of the chain termination reaction is strictly related to the reaction media: when the copolymerization was carried

[a]*Department of Chemistry, University of North Carolina at Chapel Hill, Chapel Hill, North Carolina, 27599-3290, USA. E-mail: mbrookhart@unc.edu*
[b]*Dipartimento di Scienze Chimiche, Università di Trieste, 34127, Trieste, Italy*
[c]*Department of Chemistry, University of North Carolina at Greensboro, Greensboro, North Carolina, 27412, USA*

† Electronic supplementary information (ESI) available: Descriptions of all kinetic experiments, tables of kinetic data and description of equilibrium constant measurements. Details of polymerisation experiments including NMR and GPC characterisations of copolymers, and representative ^{13}C NMR spectra showing **3a***, **4a*** and copolymer chain growth beginning with **3a***. See DOI: 10.1039/b911392d

out in methanol, nucleophilic attack of the alcohol on the Pd–acyl bond of the growing polymer chain rapidly occurred leading to polymers of very low molecular weight (M_w not higher than 20 000 Da) accompanied by fast catalyst decomposition to Pd(0);[14] when the solvent was 2,2,2-trifluoroethanol, the catalysts were remarkably stable, no alcoholysis took place and β-hydrogen elimination was the main termination process,[26] thus making feasible the synthesis of polyketones of high molecular weight, up to 10^6 Da.[13] Living CO/vinyl arene copolymerization was achieved when aprotic solvents, like CH_2Cl_2, were used.[18,19,21]

Previously, some of us reported a detailed mechanistic investigation of the key steps involved in the CO/ethylene copolymerization catalyzed by the complex [Pd(CH_3)(OEt_2)(phen)][BArF] (phen = 1,10-phenanthroline; BArF = (3,5-(CF_3)$_2$-C_6H_3)$_4$B$^-$).[20,27] The kinetic free energy barriers for the migratory insertion of carbonyl alkyl-, ethylene acyl-, and ethylene alkyl-palladium complexes as well as the relative binding constants for CO and ethylene were determined by *in situ*, low temperature NMR studies, allowing detection of key intermediates for the reaction and establishing that double ethylene insertion occurs only once in *ca.* 10^6 insertion events. The lack of double ethylene insertion events arises not only from a higher binding affinity of CO relative to ethylene but also from a significantly lower barrier for CO insertion into the palladium–alkyl bond.

NMR studies of the CO/vinyl arene copolymerization were reported by Carfagna and Nozaki. Carfagna identified key intermediates involved in the control of stereochemistry during the copolymerization process using palladium complexes containing N–N bidentate ligands like ^{i}Pr-DAB (^{i}Pr-DAB = 1,4-diisopropyl-1,4-diaza-1,3-butadiene),[28] bis-oxazoline,[29] and α-diimines.[30] Nozaki investigated Pd-complexes based on the phosphino-phosphite ligand BINAPHOS and demonstrated that, in contrast to the Pd-diphosphine systems, Pd-BINAPHOS catalyzes the CO/vinyl arene copolymerization by virtue of 1,2-regiochemistry of styrene insertion into the Pd–acyl bond.[31]

We report here an in-depth mechanistic study of the catalytic cycle of the CO/vinyl arene copolymerization catalyzed by [Pd(CH_3)(CH_3CN)(N-N)][BArF] (N-N = phen **1a**, 2,2′- bipyridine (bpy) **1b**). The structure and reactivity of key intermediates, a quantitative analysis of substituents effects in *para*-substituted styrenes, and the mechanism of chain transfer are discussed.

Results and discussion

1. Copolymerization of 4-*tert*-butyl styrene with CO

Cationic palladium complexes **1a**,**b** are excellent catalysts for the copolymerization of 4-*tert*-butylstyrene (TBS) or styrene with carbon monoxide, yielding the corresponding perfectly alternating polyketones.[18]

During TBS/CO copolymerization catalyzed by **1a**, the catalyst turnover frequency (TOF) can be assessed by measuring the rate of CO uptake under varying experimental conditions. Measuring turnover frequency at a number of different TBS concentrations shows that the rate of CO uptake is directly proportional to TBS concentration (Fig. 1), suggesting that, under standard conditions (1 atm CO at 25 °C) chain growth is first-order in the alkene. Conversely, if TBS concentration is held constant and CO pressure is increased, the rate of chain growth, as a function of monomer conversion, is inversely proportional to CO concentration.[18] This dependence is found to be inverse first-order in CO concentration as shown by a drop in the rate of polymerization by a factor of 2.70 on going from 14.7 psi CO (TOF = 0.0115 h^{-1}) to 40 psi CO (TOF = 0.0044 h^{-1}) (Fig. 2).

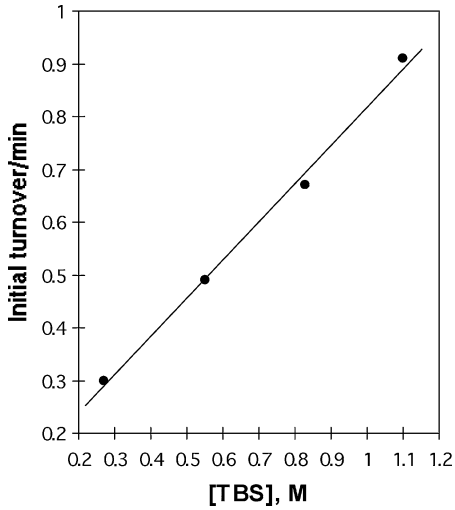

Fig. 1 Linear dependence of TOF on the concentration of TBS in the **1a**-catalyzed copolymerization of TBS/CO. TOF was a measure of CO uptake at 25 °C in CH_2Cl_2.

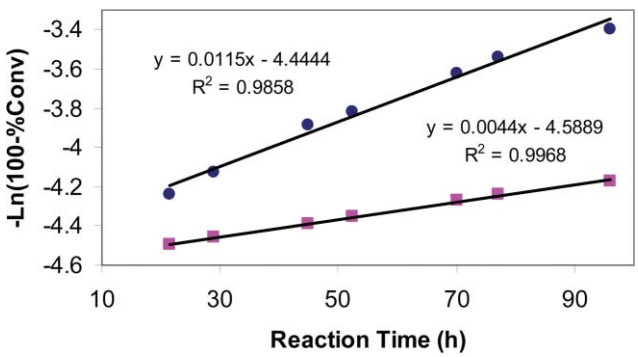

Fig. 2 Inverse dependence of TOF on the concentration of CO in the **1a**-catalyzed copolymerization of TBS/CO at 25 °C in chlorobenzene: ●14.7 psi CO; ■ 40 psi CO. k_{obs} (14.7 psi) = 0.0115 h^{-1}, k_{obs} (40 psi) = 0.0044 h^{-1}.

Changes in the alkene concentration also have an effect on the relative rates of chain propagation and chain transfer as reflected in changes in molecular weight distribution (MWD). In particular, increasing the TBS concentration resulted in broadening the MWD from near living at a low TBS concentration to 1.64 at a monomer concentration of 1.1 M (Table 1).

Table 1 TOF and MWD as a function of [TBS] for copolymerization of TBS and CO catalyzed by **1a** in CH_2Cl_2 at 25 °C under 1 atm CO

[TBS]/M	Initial TO/min	M_n	M_w/M_n
0.27	0.30	5800	1.29
0.55	0.49	12 200	1.46
0.83	0.67	13 600	1.54
1.1	0.91	13 800	1.64

The observation that chain growth in TBS/CO copolymerization is proportional to TBS concentration and inversely proportional to CO concentration is consistent with the microscopic steps of the catalytic cycle observed for the **1a**-catalyzed CO/ethylene copolymerization.[20,27] Under polymerization conditions, pre-catalyst **1a** undergoes ligand exchange with CO to form the Pd-methyl-carbonyl derivative (i), from which methyl migration occurs, generating the Pd-acyl-carbonyl intermediate (ii) (Scheme 1). This species, analogous to the corresponding derivative where the acyl fragment belongs to the growing polymer chain, represents the catalyst resting state. No acyl migration to coordinated CO occurs, since this reaction is thermodynamically unfavourable.[32,33]

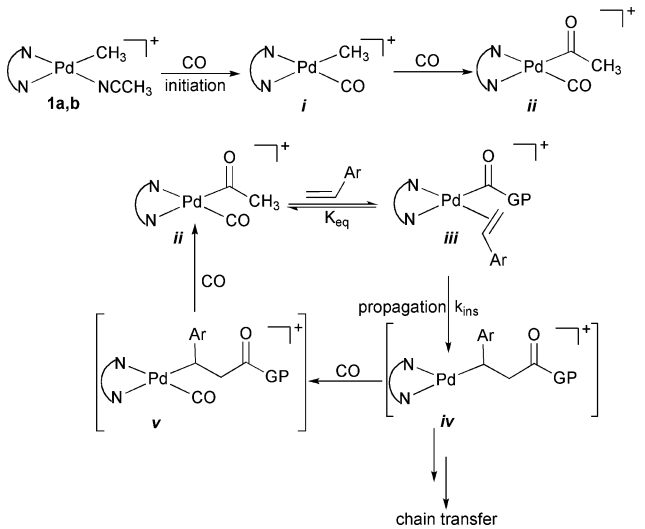

Scheme 1 General proposed mechanism for the Pd-catalyzed CO/vinyl arene copolymerization.

For propagation to proceed, the Pd-acyl-carbonyl species (ii) has to be in equilibrium with the Pd-acyl-alkene intermediate (iii), from which the migratory insertion of the olefin into the Pd–acyl bond occurs yielding the Pd-alkyl intermediate (iv). The latter can either bind CO, followed by regeneration of the resting state and completion of the catalytic cycle, or undergo β-hydrogen elimination as a chain transfer reaction leading to termination of chain growth.

The turnover frequency of a catalytic system following the mechanism depicted in Scheme 1 is given by the expression TOF = $K_{eq}k_{ins}$[TBS]/[CO]. This expression takes into account the pre-equilibrium between the resting state and the Pd-acyl-alkene species, as well as the rate of alkene insertion in the Pd-acyl complex. The two subsequent reactions, involving CO coordination and CO migratory insertion in the Pd-alkyl derivative, should be fast and are excluded from the TOF expression. This TOF expression is in accord with the observed rate dependence of polymerization on TBS and CO concentrations.

2. *In situ* NMR studies of copolymerization

(a) Observation of the Pd-acyl-carbonyl species as the catalyst resting state. The *in situ* NMR studies were performed starting from complex **5b** (Scheme 2) to avoid the presence of acetonitrile. Complex **5b** was prepared in two steps from the dialkyl

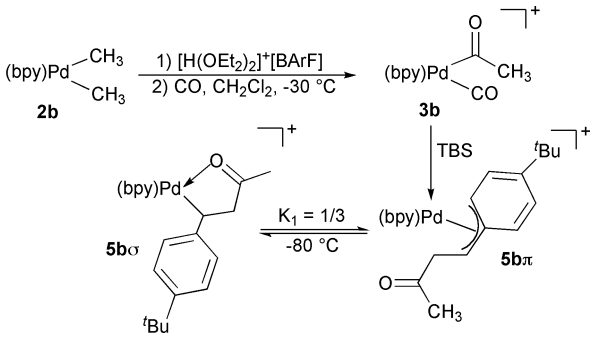

Scheme 2 Preparation of acetonitrile free pre-catalyst **5b** and its activation.

$[Pd(CH_3)_2(bpy)]$ **2b**. Protonation of **2b** with $[H(OEt_2)_2][BArF]$, at −30 °C then carbonylation yielded the Pd-acyl-carbonyl species $[Pd(C(O)CH_3)(CO)(bpy)]^+$ **3b**. (Complex **3b** can also be generated by reaction of $[Pd(CH_3)(CO)(bpy)][BArF]$ **4b**,[20] with carbon monoxide in cold CD_2Cl_2). Subsequent treatment of the cold mixture with TBS under a N_2 purge, to displace CO, gave **5b**.

Complex **5b** exists in solution as a rapidly equilibrated mixture of the chelated species $[(bpy)Pd(CHArCH_2C(O)CH_3]^+$ **5bσ** and the π-benzyl complex $[Pd(bpy)(\eta^3\text{-}CH(CH_2C(O)CH_3)Ar]^+$ **5bπ** (Scheme 2). Static ^{1}H NMR spectra, obtained at *ca.* −100 °C, indicated a **5bσ**; **5bπ** ratio of *ca.* 3 : 1. The regiochemistry of TBS insertion was studied through the preparation of a ^{13}C labelled version of **5b**, **5b***, through use of 99% ^{13}CO. The labelled carbonyl carbon displayed a $^1J_{cc}$ of *ca.* 40 Hz to both the CH_3 and CH_2 carbons in **5bσ** and **5bπ**. Such a large coupling to the methylene carbon is indicative of exclusive 2,1 TBS insertion.

Low temperature ^{13}C NMR spectroscopy of the ^{13}C-labelled carbonyl region was used to observe chain growth. An NMR sample prepared from **5b*** in CD_2Cl_2 was cooled to −78 °C then purged with ^{13}CO. Returning the sample to the probe allowed observation of the carbonyl acyl complex **6b***, as evidenced by the three characteristic carbonyl bands at 172.2, 218.7 and 207.5 ppm for the Pd–CO, the α-acyl carbonyl and $-CH_2C(O)CH_3$, respectively, to be observed (Scheme 3). The sample was removed, exposed to 6 equiv. of TBS at −78 °C and then returned to the cold probe. After 40 min, the first species detected upon insertion, at the expense of **6b***, is **7b***. After 2 h at −80 °C, **8b*** became detectable in a mixture of **6b*** and **7b***. Raising the probe to −60 °C, to hasten the polymerization, allowed **8b*** to grow as monitored by ^{13}C NMR spectroscopy.

Chemical shift assignments of the $-C(O)CH_3$ carbonyls were made after monitoring the reactions of unlabelled **5b** with ^{13}CO and TBS by ^{13}C NMR spectroscopy. Unlabelled **5b** was treated with ^{13}CO and *ca.* 10 equiv. of TBS at −78 °C. The first two insertion products, analogous to **6b*** and **7b*** but with unlabelled end groups, confirmed the assignments for $^{13}C(O)CH_3$ resonances in **6b***, **7b*** and allowed identification of the internal carbonyl resonances of **8b***. Further insertions occurred between −60 and 20 °C, which finally led to an envelope of bands in the 207–208 ppm range continually increasing in intensity relative to the Pd–CO and Pd–CO(R) bands. These experiments clearly indicate that the carbonyl acyl form of the catalyst is the catalyst resting state under these conditions.

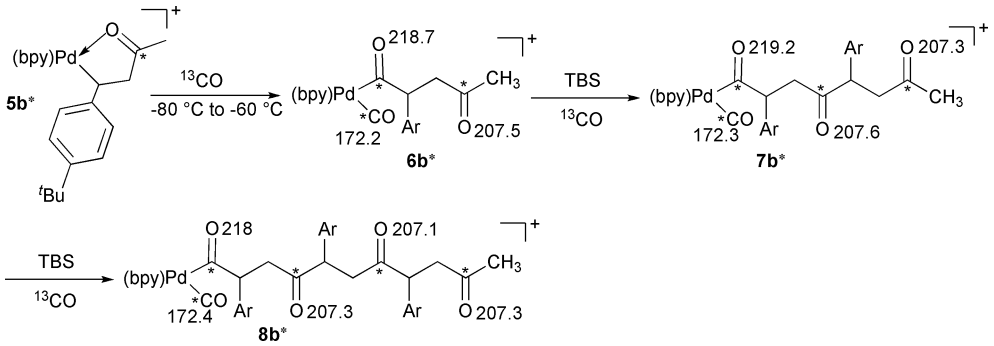

Scheme 3 ^{13}C NMR spectroscopic monitoring of sequential chain growth in the copolymerization of TBS and CO using **5b***.

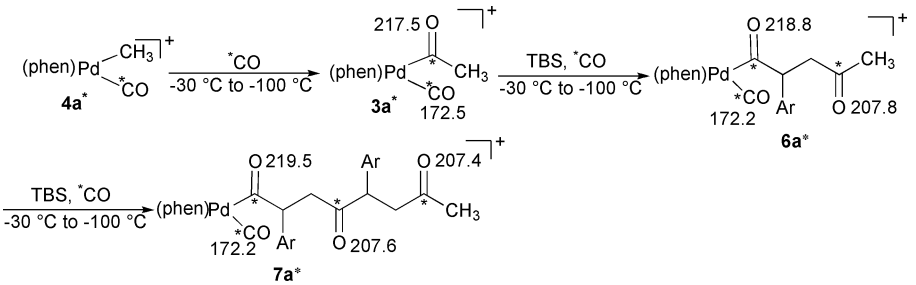

Scheme 4 ^{13}C NMR monitoring of sequential chain growth in the copolymerization of TBS and CO using **4a***.

A similar *in situ* ^{13}C NMR analysis of the copolymerization of ^{13}CO and TBS has been conducted using labelled $[Pd(CH_3)(^{13}CO)(phen)]^+$ **4a*** as the pre-catalyst (Scheme 4). Complex **4a*** was prepared *via* protonation of $[Pd(CH_3)_2(phen)]$ **2a** with $[H(OEt)_2]^+[BArF]^-$ in CH_2Cl_2 followed by a ^{13}CO purge at −78 °C.[20] Precipitation with hexanes gave colourless, analytically pure **4a***, which was used to monitor polymer chain growth.

Exposing **4a*** to ^{13}CO at −30 °C in an NMR tube and then cooling to −100 °C generated the palladium-acetyl-CO complex **3a***. When **3a*** is treated with 14 equiv. of TBS at −30 °C, followed by periodic temperature quenching of the growing polymer chain, the sequential formation of the acyl carbonyl resting state(s) **6a*** and **7a*** was monitored by NMR at −100 °C. After several insertions were observed, the sample was warmed to 20 °C in order to facilitate polymerization. Returning the sample to the cold probe resulted in observation of a broad envelope of bands at *ca.* 207 ppm as well as a new carbonyl resonance at 197 ppm. A similar resonance at 197.8 was previously observed in the ^{13}C NMR spectrum of a high molecular weight TBS/^{13}CO copolymer. This minor resonance was identified as an α,β-unsaturated enone capped polymer chain end (4-$(CH_3)_3$C-C_6H_4CH=CHC*(O)-poly). Consiglio has also identified an enone end group in the copolymerization of ^{13}C-labelled styrene with CO,[14] and the analogous end group was recognized in the CO/styrene and CO/4-Me-styrene polyketones synthesized with Pd-phenanthroline based systems in trifluoroethanol.[26]

(b) Spectroscopic observations of a palladium-acyl-alkene complex. Although the catalyst resting state for TBS/CO copolymerization, the acyl carbonyl complex, was clearly observed *via* low temperature NMR spectroscopy, the propagating palladium-acyl-alkene species was not detected. In analogy to the study performed on the migratory insertion reactions of ethylene acyl complexes,[20] a similar approach was taken in order to observe this reactive intermediate in the CO/styrene copolymerization (Scheme 5).

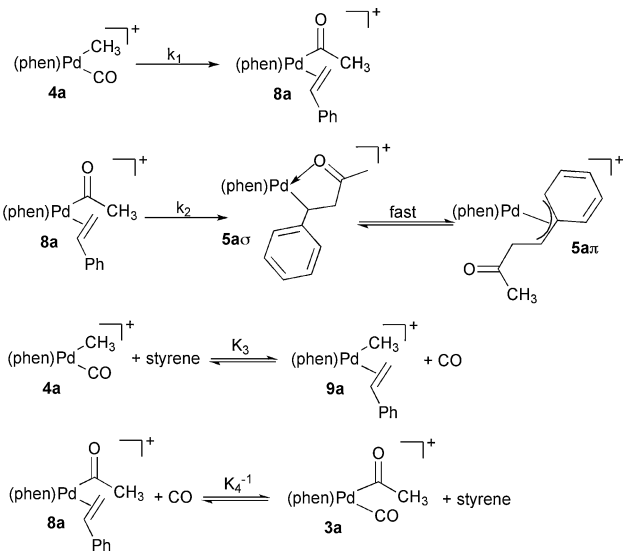

Scheme 5 Reaction scheme of **4a** with styrene.

A CD_2Cl_2 solution of **4a** was treated with 10 equiv. of styrene at −78 °C, and placed in a pre-cooled (−66 °C) NMR probe. The formation of $[Pd(C(O)CH_3)(C_6H_5CH{=}CH_2)(phen)]^+$ (**8a**) and its subsequent rearrangement, *via* acyl migration to styrene, to the equilibrated mixture of **5a**σ and π-benzyl **5a**π was observed. The two other intermediates, $[Pd(CH_3)(C_6H_5CH{=}CH_2)(phen)]^+$ (**9a**) and $[Pd(C(O)CH_3)(CO)(phen)]^+$ (**3a**), each making up less than 4% of the total composition of the reaction mixture, were also present during this experiment. The time course of the composition of the reaction is shown in Fig. 3.

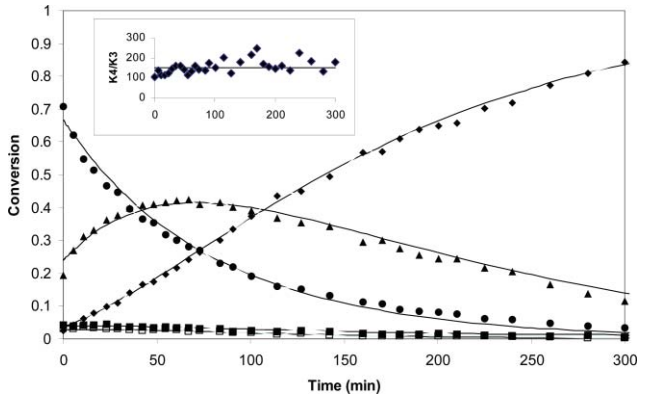

Fig. 3 Experimental and calculated composition *vs.* time data from the reaction of $[Pd(CH_3)(CO)(phen)]^+$ **4a** with styrene: ● $[Pd(CH_3)(CO)(phen)]^+$ **4a**; ▲ $[Pd(C(O)CH_3)(styrene)(phen)]^+$ **8a**; ♦ $[Pd(\eta^3\text{-}CHPhCH_2C(O)CH_3)(phen)]^+$ **5aπ**, $[Pd(CHPhCH_2C(O)CH_3)(phen)]^+$ **5aσ**; ■ $[Pd(CH_3)(styrene)(phen)]^+$ **9a**; □ $[Pd(C(O)CH_3)(CO)(phen)]^+$ **3a**. Inset is ratio of (K_4/K_3 = **[8a][4a]/[9a][3a]**) over the course of the experiment.

Consecutive migratory insertion reactions convert **4a** into **5aσ**, **5aπ** *via* **8a**. The first migratory insertion reaction of $[Pd(CH_3)(CO)(phen)]^+$ has been previously studied using different trapping agents: CO, ethylene and methyl acrylate. The evidence indicates that the insertion occurs *via* reversible methyl migration to CO followed by ligand trapping.[20] The limiting rate constant obtained in these previous studies will serve to test the numerical simulation of the data in Fig. 3. The second migratory insertion reaction converting $[Pd(C(O)CH_3)(styrene)(phen)]^+$ **8a** into the isomers **5aσ** and **5aπ**, is analogous to the previously observed first-order conversion of $[Pd(C(O)CH_3)(ethylene)(phen)]^+$ to $[Pd(CH_2CH_2C(O)CH_3)(phen)]^+$.

From Fig. 3, it is apparent that the fractions of **9a** and **3a**, while changing, are roughly the same, while the ratios **4a**/**9a** and **8a**/**3a** are not, throughout the experiment. Previous studies of ligand substitution on complex **4a** and analogues suggest that the presence of **9a** is due to styrene reacting with **4a** to yield **9a** and free CO. A large driving force for CO binding insures that the concentration of free CO is very small. Even so, the liberated CO can react with either **8a** to form **3a** or with **9a** to reform **4a**. In this manner, CO and styrene are equilibrated throughout the available sites. The roughly equivalent amounts of **9a** and **3a** suggest that the amount of CO in solution, which reacted with **5** or escaped to the head-space is very small. Thus, CO acts to couple the equilibria represented by K_3 and K_4 and as the amount of free CO available decreases, with formation of **8a** (and thus **5a**), the ratios **4a**/**9a** and **8a**/**3a** must change.

The fact that the populations of **9a** and **3a** change reveals that the equilibria are being attained at least on a similar time-scale as the insertion reactions. If either equilibrium were established slowly, then the fractions of **9a** and **3a** would be fixed. If equilibria K_3 and K_4 are fast relative to the insertions then, while the minuscule [CO] and moderate [styrene] may change, the relative equilibrium constant (K_4/K_3 = **[8a][4a]/[9a][3a]**) will be constant. A plot of K_4/K_3 *vs.* time is shown as an inset in Fig. 3. The ratio K_4/K_3 is roughly constant at 150 ± 30, while displaying a slight upward drift with an increase in scatter as the experiment progresses. A similar ordering of the relative equilibrium constants was observed in the analogous ethylene case: $K_{rel} = 34 \pm 4$.[20] In both systems, alkene binding *cis* to acetyl is favoured relative to methyl, presumably for steric reasons. The increase in scatter observed here is likely due to measuring decreasing amounts of **9a** and **3a**. The drift is possibly the result of a systematic error such as a fixed amount of impurity coincident with the resonances for **4a** or **8a**. The significance of the drift appears minor and the rapid equilibria hypothesis is consistent with the good fit obtained between the data and the mechanism in Scheme 5.

The ratio K_4/K_3 yields K_4 after determining K_3. Previous studies indirectly measured the binding affinities of styrene relative to 3,5-$(CF_3)_2$-benzonitrile ($K_A = 0.125 \pm 0.01$), and benzonitrile relative to CO ($K_B = (2.87 \pm 1.35) \times 10^{-6}$).[34] To determine K_3, the binding affinity of 3,5-$(CF_3)_2$-benzonitrile relative to benzonitrile, K_C, at −66 °C was measured: $K_C = (2.2 \pm 0.02) \times 10^{-2}$. K_3 at −66 °C is given by $K_A K_B K_C = (7.89 \pm 3.76) \times 10^{-9}$ ($\Delta G^\circ = 7.7 \pm 0.2$ kcal mol^{-1}). K_4 was then calculated from $(K_4/K_3)K_A K_B K_C$, $K_4 = (1.18 \pm 0.61) \times 10^{-6}$ ($\Delta G^\circ = 5.68 \pm 0.24$ kcal mol^{-1}) (Scheme 6).

Composition *vs.* time data were simulated numerically with the program Gear–Git.[35] The mechanism in Scheme 5 was used as the basis for calculating compositions iteratively, with changing migratory insertion rate constants, until the "best fit" with experimental data was achieved. To simplify the curve fitting, several constraints were imposed upon the calculations. Rate constants for the two equilibria were given values much larger than the insertion rate constants while maintaining the necessary ratios dictated by K_3 and K_4. Initial compositions were held at values obtained from simple exponential or biexponential fits of the data. The iterative fitting procedure then gave $k_1 = 2.32 \times 10^{-4}$ s^{-1} ($\Delta G^\ddagger = 15.4$ kcal mol^{-1}) and $k_2 = 1.47 \times 10^{-4}$ s^{-1} ($\Delta G^\ddagger = 15.6$ kcal mol^{-1}). The k_1 is in good agreement with the value determined separately from saturation kinetics experiments: $k_1(\text{sat.}) = 2.4 \pm 0.3 \times 10^{-4}$ s^{-1}.

The data obtained in this study concerning styrene binding affinities and insertion barriers combined with the previously obtained data for ethylene allows a detailed comparison of the relative insertion abilities of these monomers in phenanthroline palladium(II) systems. A free energy diagram constructed from this data is shown in Scheme 7. Facile interconversion of the alkene complexes is justified by the rapid associative ligand exchange observed previously at low temperatures. The relative insertion abilities of the two alkenes are determined by the energy differences between the transition states in accord with the Curtin–Hammett principle. Thus, while there is a lower barrier to insertion for the styrene acyl complex relative to the ethylene acyl complex, this difference is offset by ethylene's larger binding affinity. The net result is a $\Delta\Delta G^\ddagger$ of 1.2 kcal mol^{-1} favouring ethylene insertion. A similar diagram can be constructed for the methyl migratory insertion reaction. Migratory insertion from the styrene methyl complex is more favourable than the ethylene analogue, but is again offset by a larger ethylene binding affinity whose sum is a $\Delta\Delta G^\ddagger$ of 1.45 kcal mol^{-1} favouring ethylene insertion.

3. Comparison of calculated and experimental turnover frequencies for styrene/CO copolymerization

From the experimentally determined kinetic and thermodynamic data for the copolymerization of styrene and CO catalyzed by **1a**, the TOF can be predicted using the expression $TOF_{(calc)} = K_{eq} k_{ins}$[styrene]/[CO]. K_{eq} in the TOF expression is K_4 (Scheme 5)

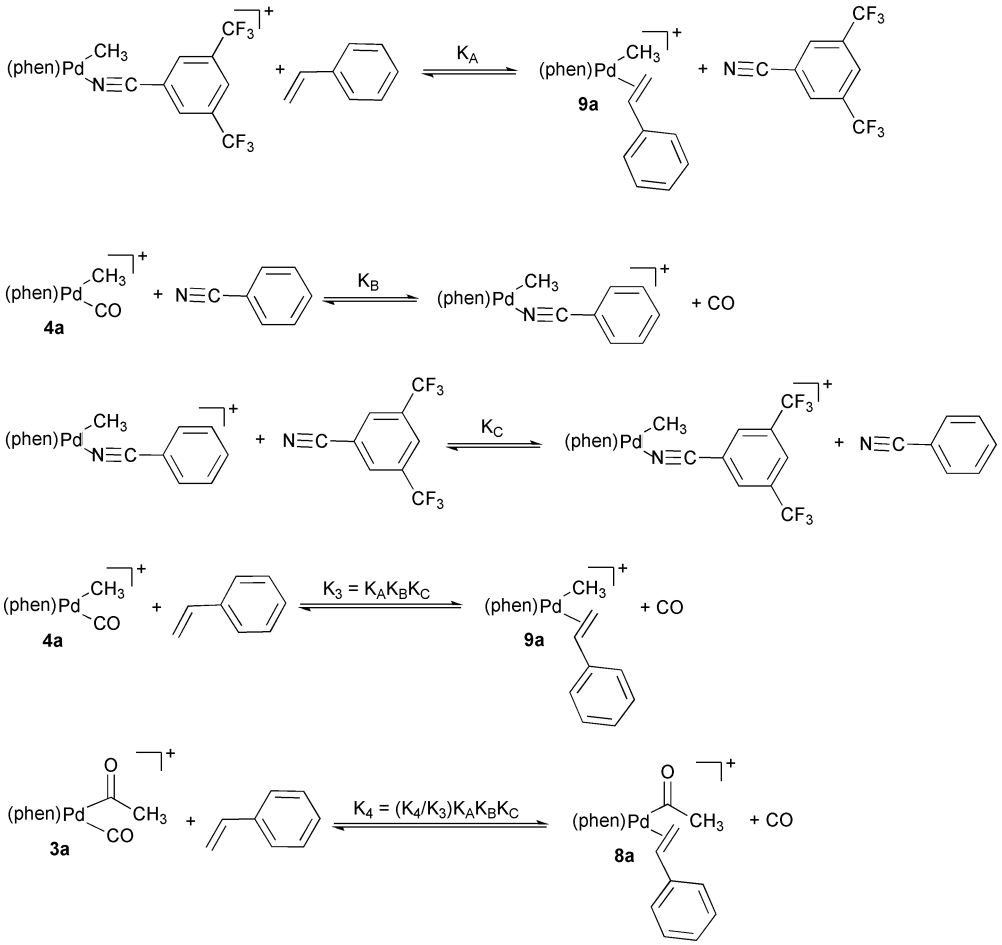

Scheme 6 Equilibria studied to determine K_3 and K_4 values.

extrapolated to 25 °C ($(2.29 \pm 2.1) \times 10^{-5}$), k_{ins} is k_2 (Scheme 5) extrapolated to 25 °C (23 ± 4 s^{-1}), [styrene] is the initial concentration of styrene in a given experiment, and [CO] is the estimated concentration of CO in the solution of styrene and CH_2Cl_2 at 25 °C (6.5×10^{-3} M).[36]‡ Using a styrene concentration of 2.9 M gives a calculated TOF of 0.23 s^{-1}. The experimentally determined TOF at this concentration is 0.011 s^{-1}. The calculated TOF is seen to overestimate the experimental TOF by roughly a factor of 20. This over approximation is not surprising when the models used to determine K_4 and k_2 are considered. For instance, the equilibrium constant is a measure of the displacement of CO by styrene in a palladium-acetyl complex (Scheme 5). Such a model does not take into account the steric bulk of the growing polymer, which will have an effect of decreasing K_4. During the copolymerization of CO with ethylene it was found that K_{eq} for ethylene binding to a palladium-acetyl-CO complex was 5 times greater than ethylene binding after just one ethylene insertion.[20] It was also noted in the ethylene/CO copolymerization that there is a 0.5 kcal mol^{-1} increase in $\Delta G^{\ddagger}$ upon changing the migrating center from acetyl to the first repeat unit. An increase in the transition state energy corresponds to a reduction in the rate of styrene insertion and therefore a smaller value for k_{ins} than k_2 predicts. If these two correction factors are used to re-estimate TOF, K_{eq} is $(1/5)K_4$ (4.58×10^{-6}) and k_{ins} is 9.7 s^{-1}, then the calculated TOF becomes 1.9×10^{-2} s^{-1}. The corrections indeed drop the estimated TOF into close approximation of the observed TOF. The ability to approximate TOF through the use of both thermodynamic and kinetic data strongly supports the proposed mechanism for the propagation of styrene/CO copolymerization.

4. Substituent effects on rate of chain growth

Having a detailed understanding of the microscopic steps in the catalytic cycle, it was of interest to examine the effects of aryl substituents on the rate of copolymerization. A series of *para*-substituted styrenes, *p*-$XC_6H_4CH{=}CH_2$ (X = –OCH_3, –CH_3, –H, –Cl) were copolymerized with CO (1 atm) at 25 °C. The TOF was determined by measuring the rate of CO uptake over the first two hours of polymerization.

Electron-rich styrenes (OCH_3, *t*Bu) were found to increase copolymerization rates, while electron-deficient styrenes (H, Cl) inhibited copolymerization. A Hammett plot of log(TOF) *vs.* σ^p gave a ρ^pexp of –0.8 for the observed turnover frequency (Fig. 4).

‡ Bryndza's calculation of [CO] compares favourably with that reported for $CHCl_3$ (8×10^{-3} M),[a,b] $ClCH_2CH_2Cl$ (6×10^{-3} M)[b]. Since [CO] in toluene is similar (7×10^{-3} M)[b] to that in CH_2Cl_2 the value of 6.5×10^{-3} M is a reasonable value for the solution of styrene and CH_2Cl_2. *(a)* W. F. Linke, Solubilities of Inorganic and Metal Organic Compounds, 4th edn, vol 1, Van Nostrand, Princeton, NJ, 1958. *(b)* W. J. Knebel and Angelici, *Inorg. Chem.*,1974, **13**, 632.

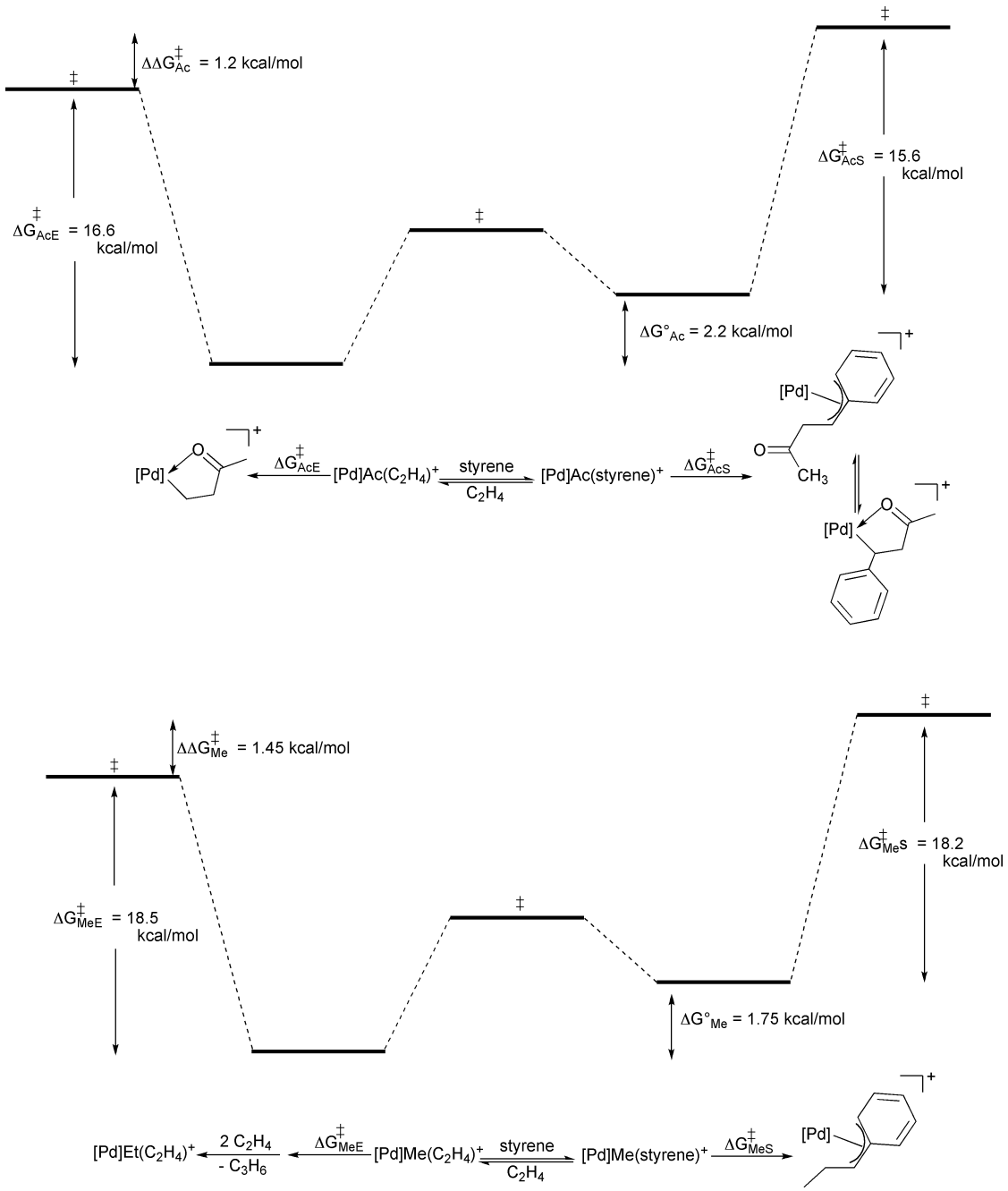

Scheme 7 Curtin–Hammett plots for migratory insertion reactions in [Pd]R(alkene)$^+$ complexes: alkene = ethylene, styrene; [Pd] = (phen)Pd; R = Me, Ac (Ac = acyl).

As shown above, the TOF = k_{poly}[styrene]/[CO], where $k_{poly} = K_{eq}k_{ins}$ (see Scheme 1). Thus, substituent effects on k_{poly} will result from effects on both K_{eq} and k_{ins} values and the ρ based on k^x_{poly} values will be the sum of $\rho(K_{eq})$ and $\rho(k_{ins})$ values. Models for both K_{eq} and k_{ins} processes are available.[20,34]

The system which best models k_{ins} is shown in eqn (2) and involves the migratory insertion of styrene methyl complex **10a** to yield π-benzyl complexes **11a**. Rix, *et. al.* showed that a Hammett plot of $\log k^x_{ins}$ *vs.* σ^p values gave a ρ^p of +1.1 ± 0.1 for these insertions.[34] This positive ρ value indicates that the rate of insertion increases as the monomer becomes more electron-deficient.

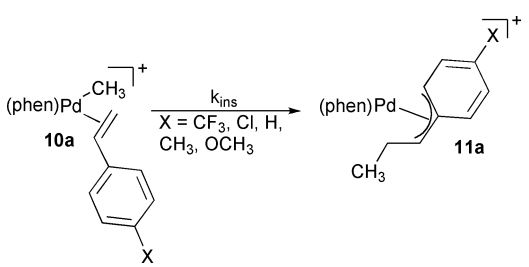

(2)

The relative binding affinities of substituted styrenes to the (phen)Pd(CH$_3$)$^+$ moiety have been previously determined and

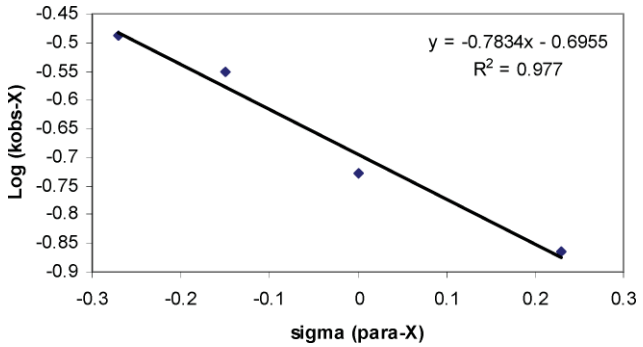

Fig. 4 Hammett plot of log (TOF) *vs.* σ^p for the rate of copolymerization of a series of substituted styrenes with CO using **1a** in CH_2Cl_2 at 25 °C.

represent an excellent model for the effect of substituents on K_{eq}(poly) (Scheme 1).[34] From observation of a series of pairwise equilibria shown in eqn (3), the relative binding affinities of substituted styrenes could be determined.

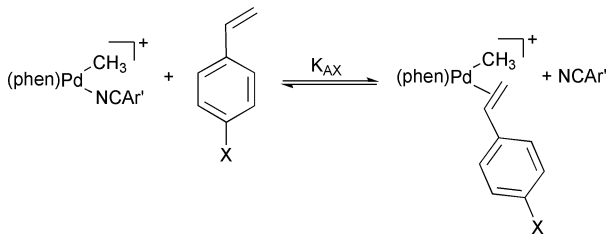

(3)

Binding affinities were shown to decrease in the order of $OCH_3 > CH_3 > H > Cl > CF_3$. In order to manipulate the K_{AX} data for a Hammett treatment, K_{BX} was found from the ratio $K_{BX} = K_{AX}/K_{AH}$ (eqn (4)). Plotting the logK_{BX} *vs.* σ^p gave a Hammett plot with a slope of $\rho^p = -2.2 \pm 0.1$. The negative slope indicates electron-rich styrenes bind more readily to the cationic palladium fragment.

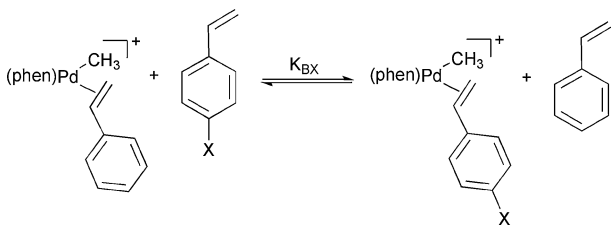

(4)

Based on the above two model systems, the predicted ρ value for the copolymerization reaction is -2.2 (K_{eq}) + 1.1 (k_{ins}) = -1.1, which is remarkably close to the experimentally determined value of -0.8. Clearly, substituent effects on the K_{eq} and k_{ins} terms oppose one another, but the dominant effect is on the K_{eq} term. Thus, the copolymerization is accelerated when the aryl substituents are electron-donating.

This finding is in agreement with experimental data reported in the literature on the CO/vinyl arene copolymerization promoted both by dicationic bischelated palladium complexes[12] $[Pd(N\text{-}N)_2][PF_6]_2$ and monocationic monochelated derivatives $[Pd(CH_3)(CH_3CN)(N\text{-}N)][PF_6]$ (N-N = phen and its substituted derivatives).[13] For all the tested catalysts, 4-Me-styrene was always found to be a more reactive alkene than styrene: higher productivities and polymers of higher molecular weight were obtained for the substituted vinyl arene with respect to styrene.

5. Mechanism of chain transfer

(a) β-Hydrogen elimination *vs.* monomer-assisted β-hydrogen abstraction leading to enone end-capped polymers. Although a reasonable understanding of the microscopic steps involved in the chain propagation of TBS/CO copolymerization exists, very little is understood about the mechanism of chain transfer in the aprotic solvent CH_2Cl_2. Three key observations have been made that must be included in any proposed chain transfer mechanism: (1) the ratio of chain transfer to chain propagation increases with increasing TBS concentration; (2) the ratio of chain transfer to chain propagation decreases with increasing carbon monoxide pressure; and (3) polymer end group analysis has shown the presence of α,β-enone end groups. Two distinct chain transfer mechanisms, each of which account for the experimental observations and share a number of common intermediates, have been proposed (Scheme 8). The most straightforward mechanism, which is consistent with recent advances from this laboratory,[34,37] is to invoke a chain transfer mechanism dependent on β-hydrogen elimination from **12** followed by associative displacement of the resulting enone **13** (pathway A, Scheme 8). Associative substitution of the enone in **13** with TBS results in free polymer bearing an enone end group and in the Pd-hydride complex **14**. Complex **14** will undergo hydride migration to TBS followed by CO coordination to generate palladium alkyl complex **15**. Complex **15** will insert CO leading to the growth of a new polymer chain through the catalyst resting state **16**. An alternative mechanism for chain transfer, again starting from the palladium alkyl complex **12**, can be envisioned, however. Complex **12**, rather than undergoing β-hydrogen elimination, can initially coordinate TBS forming palladium alkyl olefin complex **18** (pathway B, Scheme 8). Complex **18** can then undergo monomer-assisted β-hydrogen abstraction generating palladium alkyl enone **19**. Compound **19** is funnelled back into the propagating cycle after enone displacement with CO (chain transfer) forming the alkyl carbonyl species **15**.

The differences between the two types of chain transfer mechanisms outlined in Scheme 8 are subtle. For example, both mechanisms predict a decrease in the ratio of chain transfer to chain propagation rates with increasing CO concentration. As CO pressure increases, the rate of trapping of {**12**π, **12**, **12**σ} will increase and its lifetime will be decreased. Each trapping event will result in a chain extension (propagation). Thus, in either mechanism, increasing CO pressure will result in an increase in the ratio of propagation to chain transfer and a narrowing of MWD as observed experimentally (see above). Both A and B pathways can account for increasing MWD with increasing TBS concentration as this increases the ratio of chain transfer to chain propagation. In the case of pathway A if we assume {**12**π, **12**, **12**σ} is in rapid equilibrium with **13** (with equilibrium favouring {**12**π, **12**, **12**σ}) prior to formation of **14**, then the rate of chain transfer will be proportional to TBS concentration. In pathway B, TBS concentration dependence would be clearly observed for chain transfer if conversion of {**12**π, **12**, **12**σ} to **18** is either rapidly reversible favouring {**12**π, **12**, **12**σ} or if conversion of **18** to **19** is rapid relative to formation of **18** and thus trapping {**12**π, **12**, **12**σ} by TBS to form **18** is rate-determining.

Both chain transfer mechanisms depicted in Scheme 8 have been previously proposed to explain chain transfer in early transition

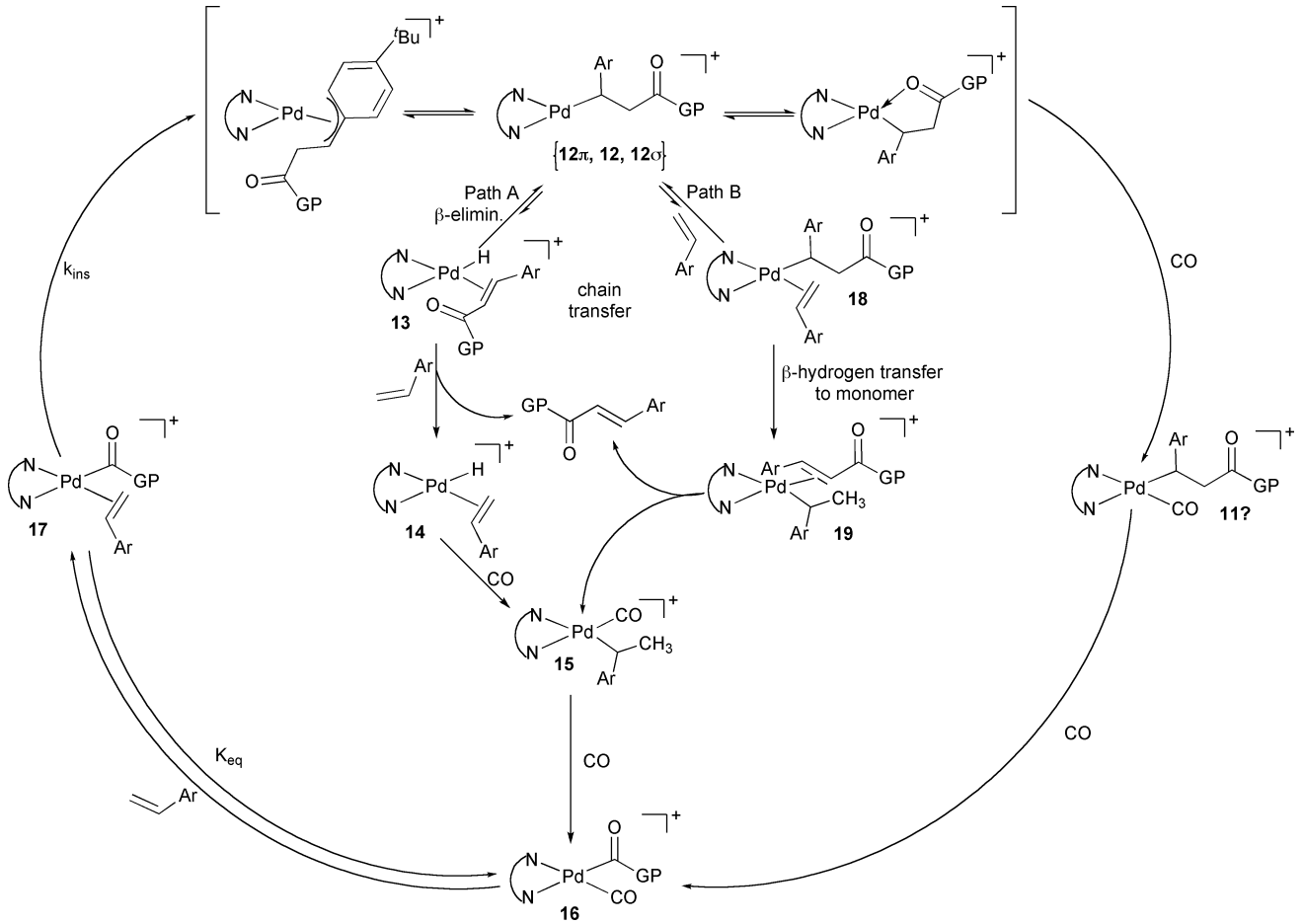

Scheme 8 Possible mechanisms describing chain transfer within the propagating catalytic cycle of TBS/CO copolymerization (GP = growing polymer).

metal catalyzed Ziegler–Natta polymerizations.[38] More recently, theoretical calculations have been performed that assess the energetic feasibility of these two pathways in late transition metal catalyzed olefin polymerizations. Calculations by Morokuma and co-workers have suggested that the β-hydrogen transfer to monomer process for chain termination in palladium diimine catalyzed ethylene polymerization would require a very large activation energy.[39] β-Hydrogen elimination followed by associative displacement appeared to be the most energetically feasible chain transfer pathway. Conversely, Ziegler and co-workers calculated that β-hydrogen elimination from a nickel diimine catalyst would be energetically unfavourable.[40,41] Their calculations indicated that chain transfer in these systems occurred by the β-hydrogen transfer to monomer mechanism. Several experiments described below were carried out in an attempt to discriminate between these two mechanisms in TBS/CO copolymerization catalyzed by **1a**.

(b) Model studies aimed at probing the mechanism of chain transfer. Complex **20a**σ,π, a model for intermediate {**12**π, **12**, **12**σ}, can be prepared by treatment of complex **1a** with CO followed by TBS as shown in Scheme 9. Treatment of **20a**σ,π with TBS results in formation of the free enone **22** and the π-benzyl complex **23** (see Scheme 10); this reaction corresponds directly to the chain transfer step. In order to gain additional information concerning this reaction a kinetic study was undertaken.

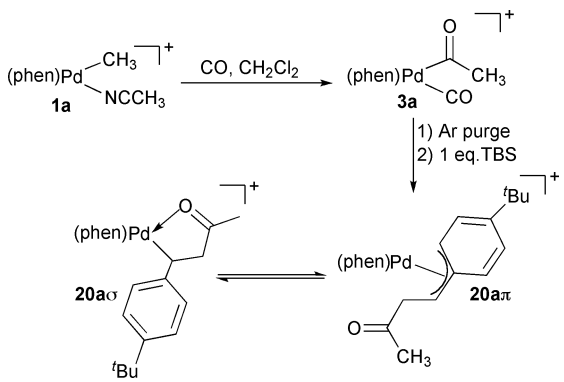

Scheme 9 Preparation of CO free palladium-alkyl **20a**.

A mechanistic scheme, which corresponds to the chain transfer step involving associative displacement (pathway A, Scheme 8), is shown in Scheme 10. Treating **21** as a steady-state intermediate, the kinetic expression for disappearance of **20a** is $-d\mathbf{20a}/dt = k_3k_4[\mathrm{TBS}][\mathbf{20a}]/(k_{-3} + k_4[\mathrm{TBS}])$. A kinetic scheme corresponding to pathway B (Scheme 8) is shown in Scheme 10. Assuming **24** never reaches significant concentrations (see below), the kinetic expression for disappearance of **20a** is $-d\mathbf{20a}/dt = k_5K_{eq}[\mathbf{20a}][\mathrm{TBS}]$. For mechanistic Scheme 10 path A, there is the possibility that at high TBS concentration k_4[TBS] will be greater than k_{-3} and thus conversion will become independent of TBS

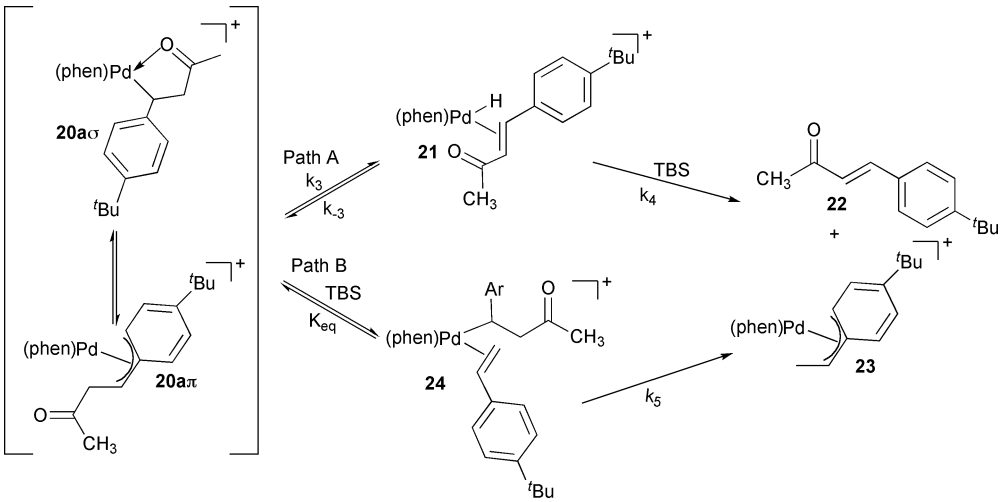

Scheme 10 Mechanism for generation of β-acetyl-4-*tert*-butylstyrene **22** from palladium-alkyl **20a**.

concentration and controlled only by rate of formation of **21** (rate = k_3[**20a**]). Therefore, kinetic experiments spanning a range of TBS concentrations may exhibit classic saturation behaviour. In contrast, Scheme 10 path B will always exhibit first-order TBS dependence (provided **24** does not build up at high TBS concentrations) with no saturation behaviour possible.

Kinetic measurements were carried out using 0.01 M solutions of **20a**σ,π in CD_2Cl_2 with added TBS in varying concentrations between 0.07 M (7 equiv.) and 1.2 M (130 equiv.). Changes in the concentration of **20a**σ,π and the liberated enone, **22**, were both monitored by integration of their respective ^{1}H NMR acyl methyl signals. Even at the highest concentration of TBS, no other palladium species besides **20a** and **23** could be detected. As can be seen from Fig. 5 a plot of k_{obs} *vs.* [TBS] is linear over the full range of TBS concentrations indicating the reaction is first-order in TBS at all concentrations. There is no evidence of saturation behaviour. Thus, the kinetic behaviour of this model is consistent with either of the two possible mechanisms shown in Scheme 10. If Scheme 10A does apply, then the linearity of Fig. 5 indicates that $k_{-3} >> k_4$[TBS] even at 1.1 M TBS.

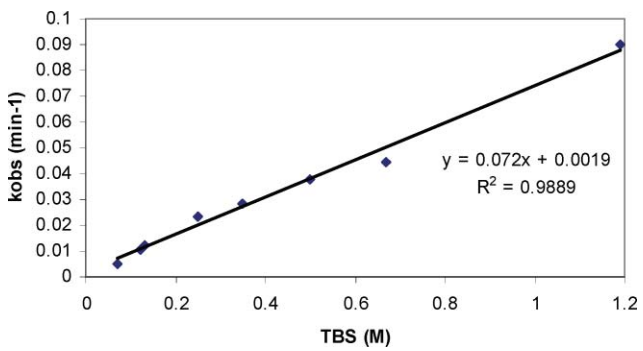

Fig. 5 Plot of k_{obs} *vs.* [TBS] for the formation of enone **22** from **20a**.

A more direct way to discriminate between a β-hydrogen elimination chain transfer mechanism and a monomer assisted β-hydrogen abstraction mechanism is through the study of the effects of added ligands on copolymerization. If the rate of chain transfer is dependent on associative displacement after β-hydrogen elimination, the addition of an external ligand capable of displacing the enone should increase the rate of chain transfer. If, on the other hand, chain transfer is independent of associative displacement, as is the case in the monomer assisted β-hydrogen abstraction mechanism, then an external ligand will have little effect on chain transfer. In order to test this hypothesis a series of TBS/CO copolymerizations catalyzed by **1a** were performed in which acetonitrile was added in varying amounts (eqn (5)). Acetonitrile was chosen as a competing ligand on both kinetic as well as thermodynamic grounds. Thermodynamically, acetonitrile has been shown to form much more stable complexes with (phen)Pd$^+$ fragments than styrene. For example, the K_{eq} for ligand exchange in the palladium styrene complex **9a** with acetonitrile was found to be *ca.* 160 at 25 °C.[42]

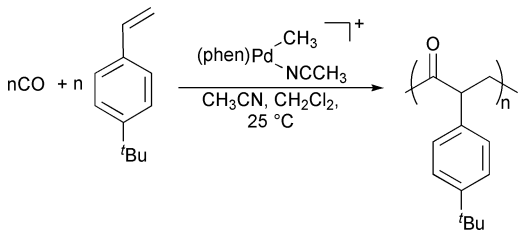

(5)

Since acetonitrile is also a smaller ligand which binds in an η^1 rather than η^2 mode, it should be kinetically very effective in displacing enone in an associative ligand displacement reaction.

In a typical experiment, 0.1 mmol of **1a** in CH_2Cl_2 were treated with 55 mmol of TBS (1.1 M) and a varying mol% of CH_3CN with respect to TBS. The homogenous reaction mixture was stirred under 1 atm of CO at 25 °C for 20 h before the white polymer was precipitated from the reaction medium through the addition of methanol. Table 2 summarizes results of the effect of varying the mol% acetonitrile in solution on the MWD of the resultant polymer. These data show that there is no significant relationship between MWD and mol% acetonitrile. In the absence of acetonitrile the copolymer produced has a MWD of 1.71. In the presence of acetonitrile, MWD varies from 1.71 at 10 mol% to 1.45 at 100 mol% additive. The lack of broadening of the MWD

Table 2 Effects of added acetonitrile on MWD and on the rate of chain propagation in a non-living copolymerization of TBS at 1.1 M and CO at 1 atm using **1a** as catalyst in CH_2Cl_2 at 23 °C

CH_3CN (mol%)	Initial TO/min	M_n	M_w/M_n
0	0.68	14 600	1.71
10	0.52	18 700	1.71
25	0.42	16 600	1.63
50	0.34	15 300	1.57
75	0.25	13 300	1.59
100	0.21	14 600	1.45

Table 3 Effects of added acetonitrile on polymer MWD in a living copolymerization of TBS at 0.27M and CO at 1 atm using **1a** as catalyst in CH_2Cl_2 at 23 °C

CH_3CN (mol%)	M_n	M_w/M_n
0	8600	1.17
10	7900	1.15
25	7200	1.13
50	6900	1.14

indicates the added ligand does not increase the rate of chain transfer. To determine the effect acetonitrile had on the rate of polymerization, CO uptake was measured over the first two hours of the reaction (Table 2). Initial TOF dropped considerably with just a few mol% of acetonitrile and dropped by as much as 70% for a 1 : 1 mixture of TBS and acetonitrile. This rate suppression is most likely an effect of acetonitrile competing with CO for binding to the acyl complex and thus reducing both the concentration of the acyl CO complex (ii) and of the palladium acyl olefin complex (iii) (Scheme 1).

The series of experiments described above were performed at a high TBS concentration in which non-living polymerization occurs. Another set of experiments were performed at lower TBS concentrations in which near-living polymerization results (Table 3). These conditions focus directly on the ability of acetonitrile to trigger chain transfer *via* enhanced associative substitution. Under the reaction conditions, TBS concentration was held constant at 0.27 M while the concentration of acetonitrile was progressively increased. The MWD of the resulting polymers precipitated after 2 h ranges only from 1.17 to 1.13 over a 50% increase in additive concentration.

Once again, acetonitrile was ineffective at increasing the rate of chain transfer. The independence of the rate of chain transfer on the concentration of acetonitrile supports a chain transfer mechanism which relies on monomer assisted β-hydrogen abstraction (pathway B, Scheme 8).§

Summary

Palladium complexes **1a** and **1b** efficiently copolymerize styrenes and CO to high molecular weight polyketones. The use of BArF as a counterion in these systems allowed for extensive ^{1}H NMR studies to be undertaken to probe the mechanism of copolymerization. A series of *in situ* polymerization monitored by NMR spectroscopy definitively showed the catalyst resting state is a palladium acyl carbonyl complex (ii) (Scheme 1). Chain propagation from (ii) was shown to be first-order in styrene concentration and inverse first order in CO concentration suggesting that TOF was dependent on a pre-equilibrium between (ii) and palladium acyl styrene complex, (iii). The equilibrium constant for the substitution of CO in the catalyst resting state by styrene was determined experimentally from palladium acyl carbonyl complex **3a** to be 2.8×10^{-7} at –66 °C. The TOF is also dependent on the rate of insertion of styrene into the palladium-acyl bond in (iii). This rate was determined by monitoring the appearance and subsequent disappearance of palladium acyl styrene complex **8a**. The rate of formation of **8a** from palladium methyl carbonyl complex **4a** was 2.3×10^{-4} s^{-1} and the rate of styrene insertion into the palladium–acetyl bond was determined to be 1.5×10^{-4} s^{-1} ($\Delta G^{\ddagger} = 15.6 \pm 0.1$ kcal mol^{-1} at –66 °C). The thermodynamic as well as kinetic data collected in the model studies was used to calculate an expected TOF for styrene/CO copolymerization from TOF(calc) = $K_{eq}k_{ins}$[styrene]/[CO] of 1.9×10^{-2} s^{-1}. The experimentally determined TOF was found to be 1.1×10^{-2} s^{-1}, which is in good agreement with the calculated value.

The dependence of TOF on both the pre-equilibrium term K_{eq} and the rate of styrene insertion (k_{ins}) was experimentally established through a Hammett treatment of the copolymerization. Styrenes substituted in the *para* position showed a linear correlation between σ^p and both K_{eq} and k_{ins}. Electron donating groups were found to increase K_{eq} ($\rho^p = -2.2$) while decreasing k_{ins} ($\rho^p = 1.1$) predicting a ρ^p for copolymerization of –1.1. The experimentally determined ρ^p value for the copolymerization of CO with a series of substituted styrenes was found to be –0.8 supporting the validity of the combined rate expression.

The mechanism of chain transfer in TBS/CO copolymerization was also probed experimentally. Chain transfer was found to increase with TBS concentration and decrease with CO pressure. Two mechanisms consistent with these observations, β-hydrogen elimination/associative substitution and monomer assisted β-hydrogen abstraction, were envisioned to both be possible from an alkyl intermediate. Data from *in situ* ^{1}H NMR kinetic experiments on formation of enone from model complex **20aσ,π** were consistent with either mechanism. However the monomer assisted β-hydrogen abstraction mechanism was supported through the study of additive effects on the rate of chain transfer. Addition of acetonitrile, which was shown to efficiently compete with styrene for binding at the metal center, had no effect on the rate of chain transfer. The inability of acetonitrile to trigger chain transfer supports a mechanism in which styrene assisted β-hydrogen abstraction is favoured over β-hydrogen elimination/associative substitution.

Experimental

General comments

All reactions, except where indicated, were carried out in flame dried glassware under a dry, oxygen-free argon atmosphere using standard Schlenk and drybox techniques. Non-deuterated solvents

§ Similar to the arguments made for the possible effects of added CH_3CN, one could propose that CO should also function as an excellent ligand for displacement of enone from **21** in the pathway A mechanism, Scheme 8. Therefore (provided formation of **13** is not rate-limiting) both trapping and chain transfer should show a first-order dependence on [CO] and thus no effect on MWD should result from changes in CO concentration. Using this analysis, the simple observation that MWD narrows with increasing [CO] itself supports pathway B for chain transfer.

were distilled under a nitrogen atmosphere from a drying agent immediately prior to use: CH_2Cl_2 from P_4O_{10}; hexanes and diethyl ether from sodium benzophenone ketyl. Acetonitrile was deoxygenated and dried *via* passage over a column of activated alumina.[43] CD_2Cl_2 and $CDCl_2F$ were dried over CaH_2, submitted to 5 freeze pump thaw cycles and then vacuum transferred into glass Schlenk tubes fitted with Kontes high vacuum Teflon plugs, and then stored under Ar. CP grade CO was purchased from National Welders Supply and used as received. 4-*Tert*-butylstyrene was generously donated by Deltech and stored under Ar over molecular sieves. Styrene, 4-chlorostyrene, and 4-vinylanisole were used as received from Aldrich.

IR spectra were recorded on a Mattson-Polaris FT-IR Spectrophotometer. ^{1}H NMR spectra were recorded on Varian XL400, Bruker AMX300, Bruker WM250 at 400, 300, 250 MHz, respectively. ^{13}C NMR were recorded on a Varian XL400 and Bruker AMX300 at 100 and 75 MHz, respectively. ^{1}H and ^{13}C chemical shifts were referenced to residual ^{1}H signals and to the ^{13}C signals of the deuterated solvents, respectively. In the ^{1}H NMR data, s, br s, d, dd, br d, br dd, br t, m, q and oct refer to singlet, broad singlet, doublet, double doublet, broad doublet, broad double doublet, broad triplet, multiplet, quartet, octet.

NMR probe temperatures were measured using an anhydrous methanol sample except for temperatures below −95 °C, which were determined using a thermocouple.

Atom labelling schemes for the phenanthroline, bipyridine and BArF counterion resonances are as follows:

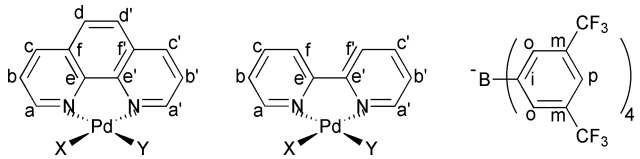

The ^{1}H NMR resonances were assigned into groups of a, b, c, d, f or a′, b′, c′, d′, f′ according to their characteristic coupling patterns. The ^{13}C NMR resonances were assigned in pairs such as C_a or $C_{a'}$ and $C_{a'}$ or C_a, based on their chemical shifts and $^1J_{CH}$. The relation between the ^{1}H and ^{13}C assignments and the stereochemistry with respect to the ligands X,Y has not been ascertained.

Errors reported for rate constants determined by kinetics are the standard deviations of several runs. Errors in $\Delta G^{\ddagger}$, $\Delta H^{\ddagger}$ and $\Delta S^{\ddagger}$ were calculated based on the derivations by Binsch and Girolami, respectively, and also incorporated $a \pm 1°$ error in temperature.[44,45] Values for σ^p were taken from March's text.[46]

C, H, N analyses were performed by Oneida Research Laboratories of Whitesboro, NY.

$[H^+(OEt_2)_2][BarF]$,[47] $CDCl_2F$,[48] $[Pd(CH_3)_2(TMEDA)]$,[49] $[Pd(CH_3)_2(phen)]$,[34] $[Pd(CH_3)_2(bpy)]$,[49] $[Pd(CH_3)Cl(COD)]$,[50] $[Pd(CH_3)Cl(bpy)]$,[51] $[Pd(CH_3)(CO)(bpy)][BArF]$,[20] $[Pd(CH_3)(CO)(phen)][BArF]$,[20] $[Pd(C(O)CH_3)(CO)(phen)][BArF]$,[20] were prepared according to literature procedures.

I. Preparations

$[Pd(CH_3)(NCCH_3)(phen)][BArF]$ (1a). $[Pd(CH_3)_2(phen)]$ (31.6 mg, 0.1 mmol) was dissolved in dry acetonitrile (10 mL) in a Schlenk tube under a N_2 atmosphere, and while this solution was stirred, $[H^+(OEt_2)_2][BArF]$ (110 mg, 1.09×10^{-4} mol) in acetonitrile (10 mL) was added over a 10 min period. After addition was complete, the reaction mixture was stirred for an additional 5 min; then excess acetonitrile was removed at reduced pressure. The product obtained in this way appeared as an air-stable, colourless or pale-yellow glass, which could be converted to a solid by tituration with toluene. An analytical sample was obtained by repeated washing with toluene and drying for 24 h *in vacuo*. Found: C 47.26, H 2.38, N 3.35. $C_{47}H_{26}BF_{24}N_3Pd$ requires C 46.81, H 2.17, N 3.48. (1,10-Phenanthroline)$Pd(CH_3)_2$ (31.6 mg, 0.1 mmol) was dissolved in dry acetonitrile (10 mL) in a Schlenk tube under a N_2 atmosphere, and while this solution was stirred, $H^+(OEt_2)_2Ar'_4B^-$ (110 mg, 1.09×10^{-4} mol) in acetonitrile (10 mL) was added over a 10 min period. After addition was complete, the reaction mixture was stirred for an additional 5 min then excess acetonitrile was removed at reduced pressure. The product obtained in this way appeared as an air-stable, colourless or pale-yellow glass, which could be converted to a solid by titration with toluene. An analytical sample was obtained by repeated washing with toluene and drying for 24 h *in vacuo*. Anal. calcd for $C_{47}H_{26}BF_{24}N_3Pd$: C 46.81, H 2.17, N 3.48. Found: C 47.26, H 2.38, N 3.35. IR (CD_2Cl_2) $\nu_{CN} = 2326$ cm^{-1}. ^{1}H NMR (250 MHz, CD_2Cl_2, 20 °C) δ 8.89 (1 H, dd, H_a), 8.81 (1 H dd, $H_{a'}$), 8.62 (2 H, m), 8.03 (2 H, AB q,), 7.92 (2 H, oct,), 7.74 (8 H, br t, Ar′-H_o), 7.56 (4 H, s, Ar′-H_o), 2.52 (3 H, s, CH_3CN), 1.28 (3 H, s, Pd-CH_3). ^{13}C NMR (100 MHz, CD_2Cl_2, 20 °C) δ 162.1 (q, J_{CB} = 50 Hz, Ar′-C_i), 149.6 (d, $J_{CH} = 179$ Hz, C_a or $C_{a'}$), 148.8 (d, J_{CH} = 183 Hz, $C_{a'}$ or C_a), 148.3 (s, C_e or $C_{e'}$), 144.4 (s, $C_{e'}$ or C_e), 140.2 (d, $J_{CH} = 167$ Hz, C_c or $C_{c'}$), 139.5 (d, $J_{CH} = 167$ Hz, $C_{c'}$ or C_c), 135.2 (d, $J_{CH} = 159$ Hz, Ar′-C_o), 131.2 (s, C_f or $C_{f'}$), 130.6 (s, $C_{f'}$ or C_f), 129.3 (q, $^2J_{CF} = 31$ Hz, Ar′-C_m), 128.1 (d, $J_{CH} = 167$ Hz, C_d or $C_{d'}$), 127.9 (d, $J_{CH} = 169$ Hz, $C_{d'}$ or C_d), 126.2 (d, J_{CH} = 169 Hz, C_b or $C_{b'}$), 125.7 (d, $J_{CH} = 171$ Hz, $C_{b'}$ or C_b), 125.0 (q, $^1J_{CF} = 272$ Hz, CF_3), 122.6 (q, $^2J_{CH} = 10$ Hz, CH_3CN), 117.9 (d, $J_{CH} = 164$ Hz, Ar′-C_p), 3.9 (q, $J_{CH} = 138$ Hz, CH_3), 3.4 (q, J_{CH}= 136 Hz, CH_3).

Alternative procedure for the preparation of **1a**: a flame dried Schlenk flask was charged with 1.97 g (5.85 mmol) of $[Pd(CH_3)(Cl)(phen)]$, prepared similarly as $[Pd(CH_3)Cl(bpy)]$,[48,51] and suspended in 50 mL of CH_2Cl_2. The suspension was then transferred by cannula to a solution of 5.93 g (1.1 equiv.) of [Na][BArF] and CH_3CN (3 mL) in 40 mL CH_2Cl_2. After stirring for 3 h at room temperature, a yellow cloudy suspension (NaCl) remains. The solution was filtered through Celite and a yellow glass remained following solvent removal *in vacuo*. The glass was washed three times with hexane to give a cream coloured foam isolated in 87% yield (4.70 g). The ^{1}H and ^{13}C NMR spectra were identical to **1a** prepared above.

$[Pd(CH_3)(NCCH_3)(bpy)][BArF]$ (1b). Complex **1b** was prepared in the same manner as its phenanthroline analog **1a** from solutions of $[Pd(CH_3)_2(bpy)]$ (29.2 mg, 0.1 mmol) in dry acetonitrile (10 mL) and $[H^+(OEt_2)_2][BArF]$ (110 mg 1.1×10^{-4} mol) in acetonitrile (10 mL). Found: C 46.31, H 2.16, N 3.12. $C_{45}H_{26}BF_{24}N_3Pd$ requires C 45.73, H 2.22, N 3.56. IR (CD_2Cl_2) $\nu_{CN} = 2328$ cm^{-1}. ^{1}H NMR (400 MHz, CD_2Cl_2, 20 °C) δ 8.58 (1 H, d, $J = 5.5$ Hz, H_a or $H_{a'}$), 8.52 (1 H, d, $J = 4.5$ Hz, $H_{a'}$ or H_a), 8.06 (4 H, m, H_f, $H_{f'}$, H_c, $H_{c'}$), 7.92 (8 H, s, Ar′-H_o), 7.69 (4 H, s, Ar′-H_p), 7.56 (2 H, m, H_b, $H_{b'}$), 2.44 (3 H, s, CH_3CN), 1.14 (3 H, s, Pd-CH_3). ^{13}C NMR (100 MHz, CD_2Cl_2, 20 °C) δ 162.5 (q, J_{CB} = 50 Hz, Ar′-C_i), 157.8 (s, C_e or $C_{e'}$), 153.2 (s, $C_{e'}$ or C_e), 149.7 (d,

J_{CH} = 184 Hz, C_a or $C_{a'}$), 148.8 (d, J_{CH} = 184 Hz, C_a or $C_{a'}$), 140.9 (d, J_{CH} = 169 Hz, C_c or $C_{c'}$), 140.7 (d, J_{CH} = 168 Hz, $C_{c'}$ or C_c), 135.5 (d, J_{CH} = 159 Hz, Ar′-C_p), 129.7 (q, $^2J_{CF}$ = 31.6 Hz, Ar′-C_m), 127.8 (d, J_{CH} = 170 Hz, C_f or $C_{f'}$), 127.5 (d, J_{CH} = 170 Hz, $C_{f'}$ or C_f), 125.3 (q, $^1J_{CF}$ = 272 Hz, CF_3), 123.7 (d, J_{CH} = 167 Hz, C_b or $C_{b'}$), 120.8 (d, J_{CH} = 166 Hz, $C_{b'}$ or C_b), 122.6 (q, $^2J_{CH}$ = 10 Hz, H_3C-*C*N), 118.2 (d, J_{CH} = 164 Hz, Ar′-C_p), 3.8 (q, J_{CH} = 136 Hz, Pd-CH_3 or CH_3CN), 3.5 (q, J_{CH} = 138 Hz, CH_3CN or Pd-CH_3).

[Pd(C(O)CH$_3$)(CO)(bpy)][BArF] (3b). An NMR tube was charged with [Pd(CH_3)(CO)(bpy)][BArF] (**4b**) (*ca.* 100 mg, 8.5 × 10^{-5} mol) and CD_2Cl_2 (0.9 mL) then purged with CO at −78 °C for *ca.* 15 min. The conversion to **3b** was observed spectroscopically, some precipitation was observed.

IR (CH_2Cl_2) ν_{CO} = 2128 (PdCO), 1746 (PdC(O)CH_3) cm^{-1}. ^1H NMR (400 MHz, CD_2Cl_2, −80 °C) δ 8.33 (1 H, d, J = 5.1 Hz, $H_{a'}$ or H_a), 8.15 (1 H, d, J = 5.3 Hz, H_a or $H_{a'}$) 7.8 (4 H, m, H_f, $H_{f'}$, H_c, $H_{c'}$), 7.78 (8 H, s, Ar′-H_o), 7.57 (1 H, m, $H_{b'}$ or H_b) 7.51 (4 H, s, Ar′-H_p), 7.46 (1 H, m, H_b or $H_{b'}$), 2.77 (3 H, s, CH_3). ^{13}C NMR (100 MHz, CD_2Cl_2, −80 °C) δ 217.4 (s, Pd*C*(O)CH_3), 172.5 (s, PdCO), 161.5 (q, $^1J_{CB}$ = 50 Hz, Ar′-C_i), 154.3 (s, C_e or $C_{e'}$), 151.6 (s, $C_{e'}$ or C_e), 150.7 (d, J_{CH} = 183 Hz, C_a or $C_{a'}$), 150.3 (d, J_{CH} = 191 Hz, $C_{a'}$ or C_a), 141.9 (d, J_{CH} = 170 Hz, C_c or $C_{c'}$), 141.2 (d, J_{CH} = 169 Hz, $C_{c'}$ or C_c), 134.3 (d, J_{CH} = 158 Hz, Ar′-C_o), 128.3 (q, $^2J_{CF}$ = 35 Hz, Ar′-C_m), 127.8 (d, J_{CH} = 185 Hz, C_f or $C_{f'}$), 127.7 (d, J_{CH} = 181 Hz, $C_{f'}$ or C_f), 124.0 (q, $^1J_{CF}$ = 273 Hz, CF_3), 123.1 (d, J_{CH} = 168 Hz, C_b or $C_{b'}$), 122.8 (d, J_{CH} = 167 Hz, $C_{b'}$ or C_b), 117.2 (d, J_{CH} = 165 Hz, Ar′-C_p), 40.6 (q, J_{CH} = 132 Hz, CH_3).

[Pd(^13^C(O)CH$_3$)(^13^CO)(bpy)][BArF] (3b*). An NMR tube charged with [Pd(CH_3)(^{13}CO)(bpy)][BArF] in CD_2Cl_2 was briefly purged with ^{13}CO (99%) at −78 °C to give **3b***. The spectroscopic data was identical to **3b** except for: IR (CH_2Cl_2) $\nu_{^{13}CO}$ = 2079 (Pd^{13}CO), 1705 (Pd^{13}C(O)CH_3) cm^{-1}. ^1H NMR (400 MHz, CD_2Cl_2, −80 °C) δ 2.77 (3 H, d, $^2J_{CH}$ = 5.9 Hz, CH_3). $^{13}C\{^1H\}$ NMR (100 MHz, CD_2Cl_2, −80 °C) δ 40.6 (dd $^1J_{CC}$ = 30 Hz, $^3J_{CC}$ = 11 Hz, CH_3).

[Pd(η^3-CH(CH$_2$C(O)CH$_3$)C$_6$H$_4$-*p*-C$_4$H$_9$)(bpy)][BArF] (5bπ), [Pd(CH(CH$_2$C(O)CH$_3$)C$_6$H$_4$-*p*-C$_4$H$_9$)(bpy)][BArF] (5bσ). [H^+(OEt_2)$_2$][BArF] (1.00 g, 9.84 × 10^{-4} mol) in CH_2Cl_2 (15 mL) was slowly syringed onto a bright yellow slurry of [Pd(CH_3)$_2$(bpy)] (**2b**) (288 mg, 9.84 × 10^{-4} mol) in CH_2Cl_2 (30 mL) giving a yellow-orange solution at −30 °C. The temperature was maintained at −30 °C while the solution was stirred for 1 h, then purged with CO for 45 min. The presence of **3b** (ν_{CO} = 2128, 1746 cm^{-1}) was verified by IR spectroscopy. After cooling the solution to −78 °C, it was purged with N_2 for 1 h to remove dissolved CO, then 1 equiv. of 4-*tert*-butylstyrene solution (9.84 × 10^{-4} mol in 4.6 mL CH_2Cl_2) was added. The N_2 purge was continued as the reaction was warmed to −30 °C for 1 h and then to 0 °C for 1 h. The small amount of black precipitate that formed upon warming was removed by filtration through Celite. The filtrate was reduced under vacuum at 0 °C to a bright yellow glass. Triturating with hexane, then drying *in vacuo* gave a brittle yellow glass which was crushed to a yellow powder (910 mg, 6.85 × 10^{-4} mol, 70% yield).

Found: C 50.83, H 2.71, N 1.97. $C_{56}H_{41}F_{24}O_1N_2Pd$ requires C 51.14, H 3.14, N 2.13. IR (CH_2Cl_2) ν_{CO} = 1719 (**5bπ**), 1617 (sh, **5bσ**) cm^{-1}. Labelling scheme:

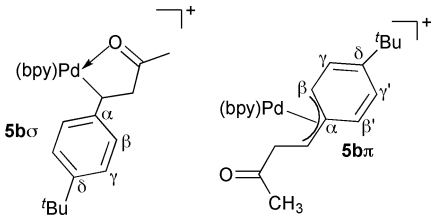

^1H NMR (400 MHz, CD_2Cl_2, 20 °C) δ 8.40 (1 H, d, J = 4.8 Hz, H_a or $H_{a'}$), 8.31 (1 H, d, J = 4.8 Hz, $H_{a'}$ or H_a), 8.06 (4H, m, H_f, $H_{f'}$, H_c, $H_{c'}$), 7.72 (8 H, s, Ar′-H_o), 7.55 (4 H, s, Ar′-H_p), 7.54 (2 H, m, H_b, $H_{b'}$), 7.50 (2 H, d, J = 8 Hz, H_b or H_g), 7.12 (2 H, d, J = 8 Hz, H_g or H_b), 3.94 (1 H, dd, J = 7.4 Hz, J = 5.0 Hz, CH_x), 3.08 (1 H, AB dd, J = 19.8 Hz, J = 7.4 Hz, CH_AH_B), 2.96 (1 H, AB dd, J = 19.8 Hz, J = 5.0 Hz, CH_AH_B), 2.44 (3 H, s, CH_3), 1.34 (9 H, s, C(CH_3)$_3$). ^1H NMR (400 MHz, $CDCl_2F$, −101 °C) δ 6.91 (1 H, d, J = 7.2 Hz, π-$H_{b'}$), 6.64 (1 H, d, J = 6.4 Hz, π-H_b), 3.8 (1 H, broad resonance ($W_{1/2}$ = 20 Hz, π-H), 3.60 (3 H, d, J = 7.2 Hz, σ-CH), 3.51 (3 H, dd, J = 19 Hz, J = 7 Hz, σ-CH_2), 3.16 (1 H, broad, J = 19.5 Hz, π-CH_2), 2.91 (1 H, dd, J = 19.5 Hz, J = 10 Hz, π-CH_2), 2.85 (3 H, d, J = 19 Hz, σ-CH_2), 2.62 (9 H, s, σ-CH_3), 2.33 (3 H, s, π-CH_3), 1.36 (9 H, s, π-C(CH_3)$_3$), 1.24 (27 H, s, σ-C(CH_3)$_3$). The remaining aromatic resonances form a complex series of multiplets in the range of 8.8 to 7.1 ppm. The resonances were referenced to residual methylene chloride at 5.32 ppm.

An equilibrium constant was determined to be *ca.* 3 to 1 from the ratio of **5bσ** to **5bπ** resonances in the −101 °C ^1H NMR spectrum.

^{13}C NMR (100 MHz, CD_2Cl_2, −80 °C) δ 238.4 (s, σ-CO), 204.5 (s, π-CO), 161.5 (q, $^1J_{CB}$ = 50 Hz, Ar′-C_i), 155.6 (s, σ-C_e or σ-$C_{e'}$), 154.8 (s, π-C_e or π-$C_{e'}$ or π-C_d), 153.9 (s, π-$C_{e'}$ or C_e or π-C_e), 152.8 (C_e or π-C_e or π-$C_{e'}$), 151.9 (d, J_{CH} = 186 Hz, π-C_a or π-$C_{a'}$), 151.3 (s, σ-C_e or σ-$C_{e'}$), 150.6 (d, J_{CH} = 187 Hz, σ-C_a or σ-$C_{a'}$), 148.4 (d, J_{CH} = 185 Hz, σ-$C_{a'}$ or σ-C_a), 148.4 (s, σ-C_a), 147.7 (d, J_{CH} = 183 Hz, π-$C_{a'}$ or π-C_a), 143.4 (s, σ-C_a), 139.9 (d, J_{CH} = 170 Hz, σ-C_c and σ-$C_{c'}$), 134.3 (d, J_{CH} = 158 Hz, Ar′-C_o), 130.4 (d, J_{CH} = 157 Hz, π-C_g or π-$C_{g'}$), 129.8 (d, J_{CH} = 153 Hz, π-$C_{g'}$ or π-C_g), 128.4 (q, $^2J_{CF}$ = 31 Hz, Ar′-C_p), 127.5 (d, J_{CH} = 174 Hz, π-C_f or π-$C_{f'}$), 127.2 (d, J_{CH} = 168 Hz, σ-C_f or σ-$C_{f'}$), 126.9 (d, J_{CH} = 169 Hz, σ-$C_{f'}$ or σ-C_f), 126.4 (d, J_{CH} = 169 Hz, σ-C_b), 125.0 (d, J_{CH} = 178 Hz, σ-C_g), 124.1 (q, $^1J_{CF}$ = 272 Hz, CF_3), 122.6 (d, J_{CH} = 166 Hz, σ-C_b or σ-$C_{b'}$), 122.1 (d, J_{CH} = 169 Hz, π-C_b or π-$C_{b'}$), 121.8 (d, J_{CH} = 168 Hz, σ-$C_{b'}$ or σ-C_b), 117.2 (d, J_{CH} = 165 Hz, Ar′-C_p), 114.7 (s, π-C_a), 107.9 (d, J_{CH} = 165 Hz, π-$C_{a'}$), 104.2 (d, J_{CH} = 172 Hz, π-C_a), 56.7 (t, J_{CH} = 127 Hz, σ-CH_2), 52.0 (d, J_{CH} = 160 Hz, π-C), 44.0 (d, J_{CH} = 141 Hz, σ-CH), 42.9 (t, J_{CH} = 125 Hz, π-CH_2), 35.5 (s, π-C(CH_3)$_3$), 34.2 (s, σ-C(CH_3)$_3$), 30.2 (q, J_{CH} = 125 Hz, σ-C(CH_3)$_3$), 29.9 (q, J_{CH} = 127 Hz, π-CH_3), 29.6 (q, J_{CH} = 122 Hz, π-C(CH_3)$_3$), 28.2 (q, J_{CH} = 130 Hz, σ-CH_3). The remaining resonances for (π-$C_{f'}$ or π-C_f) and (π-$C_{b'}$ or π-C_b) may be hidden by δ 126.9 (σ-$C_{f'}$ and σ-C_f) and δ 122.6 (σ-C_b or σ-$C_{b'}$), respectively.

[Pd(η^3-CH(CH$_2$^{13}C(O)CH$_3$)C$_6$H$_4$-*p*-C$_4$H$_9$)(bpy)][BArF] (5bπ*) and [Pd(CH(CH$_2$^{13}C(O)CH$_3$)C$_6$H$_4$-*p*-C$_4$H$_9$)(bpy)][BArF] (5bσ*). Complex **5b*** was prepared similarly to **5b**, but on a smaller scale. The $^{13}C\{^1H\}$ NMR spectrum was identical to **5b** at −80 °C except for $^1J_{CC}$ couplings.

IR (CH_2Cl_2, 25 °C) $\nu_{^{13}CO}$ = 1680 (**5bπ***), 1582 (**5bσ***) cm^{-1}. $^{13}C\{^1H\}$ NMR (100 MHz, CD_2Cl_2, −80 °C) δ 56.7 (dd,

$^1J_{CC}$ = 43 Hz, **5bσ***-CH_2), 42.9 (d, $^1J_{CC}$ = 36 Hz, **5bπ***-CH_2), 26.2 (d, $^1J_{CC}$ = 40 Hz, **5bσ***-CH_3). The missing resonance for δ 29.9 (**5bπ***-CH_3) is split under the broad neighbouring peaks δ 30.2 (**5bσ***-($C(CH_3)_3$)) and δ 29.6 (**5bπ***-($C(CH_3)_3$)).

[Pd(CH(C_6H_5)CH_2C(O)CH_3)(phen)][BarF] (5aσ) and [Pd(η³-CH(CH_2C(O)CH_3)C_6H_5)(phen)][BArF] (5aπ). Styrene (17.4 μL, 1 equiv.) was added to a CH_2Cl_2 (1 mL) solution of **4a** (181 mg, 1.52×10^{-4} mol) at 20 °C. The colour turned intense yellow. After stirring briefly, the solvent was removed *in vacuo* to yield **5aσ,π** as a yellow glass (169 mg, 81%).

IR (CH_2Cl_2) ν_{CO} = 1717 (π), 1614 (σ) cm^{-1}. ^1H NMR (400 MHz, CD_2Cl_2, 20 °C) δ 8.9 (1 H, br d, H_a or $H_{a'}$), 8.54 (2 H, w, H_c and $H_{c'}$), 8.4 (1 H, br d, $H_{a'}$ or H_a), 7.99 (1 H, d, $J_{d,d'}$ = 8.8 Hz, H_d or $H_{d'}$), 7.95 (1 H, d, $J_{d,d'}$ = 8.8 Hz, $H_{d'}$ or H_d), 7.89 (1 H, dd, J= 8.2 Hz, J = 5.2 Hz, H_b or $H_{b'}$), 7.7 (9 H, m, Ar′-H_o + $H_{b'}$ or H_b), 7.55 (4 H, s, Ar′-H_p), 7.5 (1 H, m, *p*-H-C_6H_4), 7.4 (4 H, m, C_6H_4), 4.10 (1 H, dd, J_{AM} = 7 Hz, J_{BM} = 5 Hz, CH_MAr), 3.30 (1 H, dd, J_{AB} = 20 Hz, J_{AM} = 7 Hz, C$H_A$$H_B$), 3.11 (1 H, dd, J_{AB} = 20 Hz, J_{BM} = 5.0 Hz, $CH_A$$H_B$), 2.58 (3 H, s, CH_3).

Low temperature ^1H NMR revealed **5aσ**–**5aπ** = 11 : 1.

5aσ: ^1H NMR (400 MHz, CD_2Cl_2, –90 °C) δ 8.92 (1 H, br d, phen), 8.63 (1 H, br d, phen), 8.39 (2 H, m, phen), 7.8 (12 H, m, H_b and $H_{b'}$ + H_d and $H_{d'}$ + Ar′-H_o), 7.3 (2 H, m, Ph), 7.2 (3 H, m, Ph), 3.88 (1 H, br d, J = *ca.* 7.5 Hz, CHAr), 3.55 (br dd, J = 21 Hz, J = *ca.* 7.5 Hz, C*H*H), 2.94 (br d, J = 21 Hz, CH*H*), 2.63 (3 H, s, CH_3).

5aπ: ^1H NMR (400 MHz, CD_2Cl_2, –90 °C) δ 9.03 (m, phen), 8.4 (m, phen), (remainder aromatics are obscured), 7.03 (1 H, d, *ortho* H of Bz), 6.66 (1 H, d, *ortho* H of Bz), 4.5 (1 H, m, C*H*Ar), 3.2 (d, J = *ca.* 20 Hz), 2.32 (3 H, s, CH_3). The missing resonances of **5aπ** are obscured by those of the major isomer **5aσ**.

Warming the sample to –81 °C caused the methyl resonances of the two isomers to broaden significantly. The rate of conversion of the minor isomer **5aπ** into the major, **5aσ**, was determined from $k = \pi(W - W_o)$, where W = 12 Hz, W_o = 3 Hz, k = 36 Hz, $\Delta G^{\ddagger}_{min\rightarrow maj}$ = 9.7 ± 0.1 kcal mol^{-1}. Knowing K_{eq} = 11 : 1, ΔG° = 0.9 kcal mol^{-1}, gives $\Delta G^{\ddagger}_{maj\rightarrow min}$ = 10.6 ± 0.1 kcal mol^{-1}.

Trapping with Styrene. A 5 mm NMR tube was charged with **4a** (10 mg, 8×10^{-6} mol) and CD_2Cl_2 (0.7 mL). Styrene (9 μL, 10 equiv.) was added to the sample at –78 °C. The sample was briefly shaken to dissolve the frozen styrene on the inside of the tube. The sample was then placed in a pre-cooled NMR probe (–66 °C) where the conversion of **4a** to the intermediate [Pd(C(O)CH_3)(C_6H_5CH=CH_2)(phen)]$^+$ (**8a**) *en route* to **5aσ,π** was observed. The characterization of **8a** was limited because free and coordinated styrene exchange on the NMR timescale. The methyl resonances of **4a** (δ = 1.5), **8a** (δ = 2.15) and **5aσ,π** (δ = 2.65) (time averaged) and the carbonyl acyl **3a** (δ = 2.9) and the styrene methyl **9a** (δ = 0.9) were monitored with time. **8a**: ^1H NMR (300 MHz, CD_2Cl_2, –66 °C), δ 8.6 (2 H, br d, J ~ 8.5 Hz, H_c and $H_{c'}$), 8.4 (2 H, br d, J ~ 5 Hz, H_a and $H_{a'}$), 7.97 (2 H, s, H_d and $H_{d'}$), 7.9 (2 H, dd, J ~ 8.5 Hz, J ~ 5 Hz, H_b and $H_{b'}$), 2.15 (3 H, s, CH_3).

II. Polymerizations

***In situ* copolymerizations of *p*-*t*-butylstyrene with ^{13}CO. *In situ* copolymerizations of *p*-*t*-butylstyrene with ^{13}CO. [Pd(C(O)CH(*p*-C_4H_9-C_6H_4)CH_2C(O)-CH_3)(CO)(bpy)][BArF] (6b).** An NMR tube was charged with **5b** (*ca.* 100 mg, 7.5×10^{-5}mol) and CD_2Cl_2 (0.9 mL) then purged with CO at –78 °C for *ca.* 15 min. The conversion of **5b** to **6b** was observed spectroscopically.

IR (CH_2Cl_2) ν_{CO} = 2126 (PdCO), 1742 (PdC(O)–), 1715 (–C(O)CH_3) cm^{-1}. ^1H NMR (400 MHz, CD_2Cl_2, –80 °C) δ 8.45 (1 H, br s, H_a or $H_{a'}$), 8.22 (1 H, d, J = 4.92 Hz, $H_{a'}$ or H_a), 8.65 (4 H, m, H_f, $H_{f'}$, H_c $H_{c'}$), 7.73 (8 H, s, H_b), 7.57 (2 H, br s, H_b, $H_{b'}$), 7.36 (1 H, d, J = 8.0 Hz, H_b or H_g), 7.25 (1 H, d, J_{CH} = 7.8 Hz, H_g or H_b), 4.77 (1 H, d, J = 11.3 Hz, CH_2), 3.70 (1 H, dd, J = 18.4 Hz, J = 11.3 Hz, CH_2), 2.80 (1 H, d, J = 18.5, CH), 2.24 (3 H, s, CH_3). ^{13}C NMR (100 MHz, CD_2Cl_2, –80 °C) δ 218.7 (s, Pd-C(O)-CH(Ar)–), 207.5 (s, –CH_2C(O)CH_3), 172.2 (s, Pd-CO), 161.5 (q, J_{CB} = 50 Hz, Ar′-C_i), 154.1 (s, C_e or $C_{e'}$), 152.4 (s, Ar′-C_p), 152.1 (d, J_{CH} = 193 Hz, C_a or $C_{a'}$), 151.9 (s, $C_{e'}$ or C_e), 150.1 (d, J_{CH} = 188 Hz, $C_{a'}$ or C_a), 141.3 (d, J_{CH} = 168 Hz, C_c or $C_{c'}$), 141.0 (d, J_{CH} = 169 Hz, $C_{c'}$ or C_c), 129.4 (d, J_{CH} = 145 Hz, C_b or C_g), 128.8 (s, Ar′-C_i), 128.3 (q, $^2J_{CF}$ = 31 Hz), 127.4 (d, J_{CH} = 182 Hz, C_f or $C_{f'}$), 127.3 (d, J_{CH} = 182 Hz, $C_{f'}$ or C_f), 126.7 (d, J_{CH} = 157 Hz, C_g or C_b), 124.0 (q, $^1J_{CF}$ = 273 Hz, CF_3), 122.7 (d, J_{CH} = 167 Hz, C_b or $C_{b'}$), 122.6 (d, J_{CH} = 167 Hz, $C_{b'}$ or C_b), 117.2 (d, J_{CH} = 156 Hz, Ar′-C_p), 62.1 (d, J_{CH} = 137 Hz, CH), 46.1 (t, J_{CH} = 129 Hz, CH_2), 34.2 (s, $C(CH_3)_3$), 30.3 (q, J_{CH} = 126 Hz, C(CH_3)$_3$), 29.4 (q, J_{CH} = 128 Hz, C(O)CH_3).

(a) $^{13}C\{^1H\}$ NMR monitoring of chain growth:

5b* → **6b*** → **7b*** → **8b***.

Complex **5b***, prepared as described from [Pd(CH_3)$_2$(bpy)] (14.4 mg, 4.92×10^{-5} mol), was dissolved in CD_2Cl_2 (0.9 mL), then syringed into a stoppered NMR tube and cooled to –78 °C. The sample was briefly purged with ^{13}CO (99%), then placed in a cold NMR probe (–80 °C). The conversion of **5b*** to **6b*** and some [Pd(CH_3)(^{13}CO)(bpy)][BArF] to **3b***, respectively, was observed by $^{13}C\{^1H\}$ NMR spectroscopy. The sample was then removed from the NMR probe and placed in a dry ice/isopropanol bath. 4-*t*-Butyl styrene (10 μL, 5.49×10^{-5} mol, *ca.* 6 equiv., as determined spectroscopically) was syringed into the cold sample which was shaken rapidly and returned to the cold NMR probe (–80 °C). The resonances for **7b*** began to appear 40 min after the addition of olefin. After 2 h all the carbonyl resonances for **7b*** and all but one for **8b*** could be identified. The resonances of **3b*** slowly decreased in intensity.

Labelling scheme:

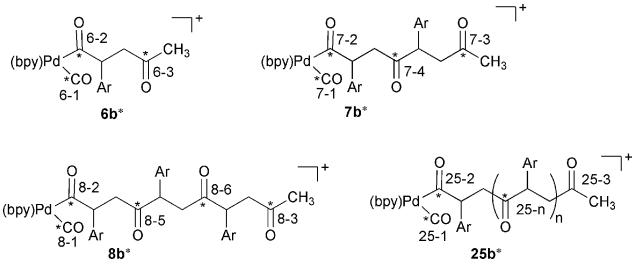

7b*: $^{13}C\{^1H\}$ NMR (100 MHz, CD_2Cl_2, –80 °C) δ 219.2 (**7**-C_2), 207.6 (**7**-C_4), 207.3 (**7**-C_3), 172.3 (**7**-C_1).

8b*: $^{13}C\{^1H\}$ NMR (100 MHz, CD_2Cl_2, –80 °C) δ 218.0 (**8**-C_2), 207.3, 207.1 (**8**-C_3, C_5 or C_6), 172.40 (**8**-C_1). Some organic carbonyl resonances are believed to be coincident with other similar resonances. After 2.5 h at –80 °C, all of **3b*** had been converted to **6b***. The temperature was then raised to –60 °C where distinct bands of resonances were observed for the

Pd-CO, PdC(O)R and organic carbonyls at slightly different chemical shifts, which are presumably temperature dependent.

$^{13}C\{^1H\}$ NMR (100 MHz, CD_2Cl_2, −60 °C) δ 218.7 (**7**-C_2), 218.3 (**6**-C_2), 217.6 (**8**-C_2), 207.7 (**6**-C_3 + **7**-C_4), 207.4 (**8**-C_5 or **8**-C_6 + **7**-C_3 + **8**-C_3), 207.2 (**8**-C_6 or **8**-C_5), 172.7 (**8**-C_1), 172.6 (**7**-C_1), 172.5 (**6**-C_1).

(b) $^{13}C\{^1H\}$ NMR monitoring of chain growth:

5b → **6b***u → **7b***u → **8b***u → **5b***u

The "u" after the compound number denotes a non-^{13}C labelled acetyl end group. **5b** was prepared on the same scale as **5b***. The procedure was similar to the previous one, except that **5b** was used instead of **5b*** and *p-t*-butyl styrene (30 μL, 1.65×10^{-4} mol, *ca.* 10 equiv. as determined spectroscopically) was used. **6b***u exhibited two carbonyl resonances: $^{13}C\{^1H\}$ NMR (100 MHz, CD_2Cl_2, −80 °C) δ 218.7 (**6**-C_2), 172.2 (**6**-C_1). **7b***u exhibited three carbonyl resonances: $^{13}C\{^1H\}$ NMR (100 MHz, CD_2Cl_2, −80 °C) δ 219.2 (**7**-C_2), 207.6 (**7**-C_4), 172.3 (**7**-C_1). After 45 min at −80 °C, the temperature was raised to −60 °C. **8b***u exhibited four carbonyl resonances: $^{13}C\{^1H\}$ NMR (100 MHz, CD_2Cl_2, −60 °C) δ 217.5 (**8**-C_2), 207.5 (**8**-C_6 or **8**-C_5), 207.2 (**8**-C_5 or **8**-C_6), 172.7 (**8**-C_1). After 2 h 45 min at −60 °C, the temperature was raised to −40 °C to induce more rapid chain growth. Extensive chain growth was verified by the appearance of the spectrum after 50 min: $^{13}C\{^1H\}$ NMR (100 MHz, CD_2Cl_2, −40 °C) δ 217.8 (weak, C_2), 207–208 (br envelope, C_n), 172.8 (weak C_1), 172.7 (weak $C_{1'}$).

The temperature was raised to 20 °C: $^{13}C\{^1H\}$ NMR (100 MHz, CD_2Cl_2, 20 °C) δ 207–208 (broad envelope).

(c) [Pd(CH$_3$)(^{13}CO)(phen)][BArF] (4a*) + ^{13}CO and TBS. A 5 mm NMR tube was charged with **4a*** (25 mg, 2×10^{-5} mol) and CD_2Cl_2 (0.7 mL). ^{13}CO was purged through the solution at −78 °C for *ca.* 20 s and the sample placed in a pre-cooled (−100 °C) NMR probe. The sample was warmed to −30 °C to increase the rate of the reaction; complex **3a*** formed and the sample was returned to −100 °C. The terminal CO of the carbonyl complex averaged with the free CO at higher temperatures in this sample. *p-t*-butyl styrene (50 μL, 2.7×10^{-4} mol, 14 equiv.) was added to the sample at −78 °C and the sample placed in the (−30 °C) NMR probe. The reaction was followed over the course of *ca.* 48 h, interrupted by one 5 h period where the sample was stored at −78 °C. Periodically the sample was cooled to −100 °C to obtain spectra of the "quenched" polymerizing system as **6a***, **7a***, *etc.*

6a*: $^{13}C\{^1H\}$ NMR (100 MHz, CD_2Cl_2, −100 °C) δ 218.8 (**6**-C_2), 207.8 (**6**-C_3), 172.2 (**6**-C_1).

7a*: $^{13}C\{^1H\}$ NMR (100 MHz, CD_2Cl_2, −100 °C) δ 219.5 (**7**-C_2), 207.6 (**7**-C_4), 207.4 (**7**-C_3), 172.2 (**7**-C_1).

[$\overline{\text{Pd(CH(}p\text{-Bu-C}_6\text{H}_4\text{)CH}_2\text{C(O)CH}_3\text{)}}$(phen)][BArF] (20aσ) and [Pd(η^3-CH(CH$_2$C(O)CH$_3$)*p*-*t*-Bu-C$_6$H$_4$)(phen)][BArF] (20bπ). A flame dried Schlenk flask was charged with 300 mg (0.249 mM) of **1a**, which is then dissolved in 15 mL CH_2Cl_2 under argon. The solution was purged with CO at room temperature for 15 min followed by an argon purge for 25 min at −80 °C. One equiv. of TBS (45.1 μL) was syringed into the Schlenk flask at −80 °C and the reaction was removed from the ice bath and stirred at room temperature for 1 h. Solvent was removed *in vacuo* leaving a yellow glass. The glass was then re-dissolved in 10 mL of toluene and solvent was removed *in vacuo* once again to insure that no free CH_3CN was present. The yellow glass, which remained, was washed three times with hexane, leaving a yellow orange powder (280 mg, 83% yield). ^1H data for **20aσ,π** at room temperature are given below.

20a: ^1H NMR (400 MHz, CD_2Cl_2, +20 °C): δ 8.7 (1 H, m, H_a or $H_{a'}$), 8.55 (2 H, d, J = 8 Hz, H_c, $H_{c'}$), 7.99 (2 H, d, J = 2 Hz, H_d, $H_{d'}$), 7.87 (1 H, dd, J = 8 Hz, J = 5 Hz, H_b or $H_{b'}$), 7.82 (1 H, dd, J = 8 Hz, J = 4 Hz, H_b or $H_{b'}$), 7.72 (8 H, s, H_o), 7.54 (4 H, s, H_p), 7.53 (2 H, d, J = 8 Hz, H_o or H_m), 7.20 (2 H, d, J = 8 Hz, H_o or H_m), 4.15 (1 H, overlapping dd, J = 6 Hz, J = 6 Hz, CH), 3.10 (2 H, dd, J = 6 Hz, J = 6 Hz, CH_2), 2.50 (3 H, s, $C(O)CH_3$), 1.36 (9 H, s, $C(CH_3)_3$).

Acknowledgements

We are grateful to the Department of Energy (FG05-94ER14459), the National Science Foundation (CHE-0615704), and DuPont for financial support of this work. F. C. R was supported in part by a Department of Education Fellowship and J. C. B. was supported by an NSF-ROA grant.

References

1 A. Sen and T.-W. Lai, *J. Am. Chem. Soc.*, 1982, **104**, 3520.
2 T.-W. Lai and A. Sen, *Organometallics*, 1984, **3**, 866.
3 E. Drent, J. A. M. van Broekhoven and M. J. Doyle, *J. Organomet. Chem.*, 1991, **417**, 235.
4 E. Drent and P. H. M. Budzelaar, *Chem. Rev.*, 1996, **96**, 663.
5 C. Bianchini and A. Meli, *Coord. Chem. Rev.*, 2002, **225**, 35.
6 K. Nakano, N. Kosaka, T. Hiyama and K. Nozaki, *Dalton Trans.*, 2003, 4039.
7 J. Durand and B. Milani, *Coord. Chem. Rev.*, 2006, **250**, 542.
8 E. J. García Suárez, C. Godard, A. Ruiz and C. Claver, *Eur. J. Inorg. Chem.*, 2007, 2582.
9 T. M. J. Anselment, S. I. Vagin and B. Rieger, *Dalton Trans.*, 2008, 4537.
10 N. Alperwicz, *Chem. Week*, 1995, 127.
11 B. Milani, A. Anzilutti, L. Vicentini, A. Sessanta, o Santi, E. Zangrando, S. Geremia and G. Mestroni, *Organometallics*, 1997, **16**, 5064.
12 A. Scarel, B. Milani, E. Zangrando, M. Stener, S. Furlan, G. Fronzoni, G. Mestroni, S. Gladiali, C. Carfagna and L. Mosca, *Organometallics*, 2004, **23**, 5593.
13 Jèrome Durand, Ennio Zangrando, Mauro Stener, Giovanna Fronzoni, Carla Carfagna, Barbara Binotti, Paul C. J. Kamer, Christian Muller, Maria Caporali, Piet W. N. M. van Leeuwen, Dieter Vogt and B. Milani, *Chem.–Eur. J.*, 2006.
14 M. Barsacchi, G. Consiglio, L. Medici, G. Petrucci and U. W. Suter, *Angew. Chem., Int. Ed. Engl.*, 1991, **30**, 989.
15 M. Barsacchi, A. Batistini, G. Consiglio and U. W. Suter, *Macromolecules*, 1992, **25**, 3604.
16 A. Aeby, A. Gsponer and G. Consiglio, *J. Am. Chem. Soc.*, 1998, **120**, 11000.
17 Giambattista Consiglio and B. Milani, in '*Stereochemical aspects of cooligomerization and copolymerization*', ed. A. Sen, Dordrecht, 2003.
18 M. Brookhart, F. C. Rix, J. M. DeSimone and J. C. Barborak, *J. Am. Chem. Soc.*, 1992, **114**, 5894.
19 M. Brookhart, M. I. Wagner, G. G. A. Balavoine and H. A. Haddou, *J. Am. Chem. Soc.*, 1994, **116**, 3641.
20 F. C. Rix, M. Brookhart and P. S. White, *J. Am. Chem. Soc.*, 1996, **118**, 4746.
21 M. Brookhart and M. I. Wagner, *J. Am. Chem. Soc.*, 1996, **118**, 7219.
22 K. Nozaki, N. Sato and H. Takaya, *J. Am. Chem. Soc.*, 1995, **117**, 9911.
23 S. Bartolini, C. Carfagna and A. Musco, *Macromol. Rapid Commun.*, 1995, **16**, 9.
24 M. T. Reetz, G. Aderlein and K. Angermund, *J. Am. Chem. Soc.*, 2000, **122**, 996.
25 A. Bastero, C. Claver, A. Ruiz, S. Castillon, E. Daura, C. Bo and E. Zangrando, *Chem.–Eur. J.*, 2004, **10**, 3747.
26 B. Milani, G. Corso, G. Mestroni, C. Carfagna, M. Formica and R. Seraglia, *Organometallics*, 2000, **19**, 3435.
27 F. C. Rix and M. Brookhart, *J. Am. Chem. Soc.*, 1995, **117**, 1137.

28 C. Carfagna, G. Gatti, D. Martini and C. Pettinari, *Organometallics*, 2001, **20**, 2175.
29 B. Binotti, C. Carfagna, G. Gatti, D. Martini, L. Mosca and C. Pettinari, *Organometallics*, 2003, **22**, 1115.
30 B. Binotti, G. Bellachioma, G. Cardaci, C. Carfagna, C. Zuccaccia and A. Macchioni, *Chem.–Eur. J.*, 2007, **13**, 1570.
31 K. Nozaki, H. Komaki, Y. Kawashima, T. Hiyama and T. Matsubara, *J. Am. Chem. Soc.*, 2001, **123**, 534.
32 J.-T. Chen and A. Sen, *J. Am. Chem. Soc.*, 1984, **106**, 1506.
33 A. Sen, J.-T. Chen, W. M. Vetter and R. R. Whittle, *J. Am. Chem. Soc.*, 1987, **109**, 148.
34 F. C. Rix, M. Brookhart and P. S. White, *J. Am. Chem. Soc.*, 1996, **118**, 2436.
35 F. Weigert, and R. McKinney, in 'Gear-Git Software'.
36 H. E. Bryndza, *Organometallics*, 1985, **4**, 1686.
37 L. K. Johnson, C. M. Killian and M. Brookhart, *J. Am. Chem. Soc.*, 1995, **117**, 6414.
38 H. Sinn and W. Kaminsky, *Adv. Organomet. Chem.*, 1980, **18**, 99.
39 D. G. Musaev, M. Svensson, K. Morokuma, S. Stromberg, K. Zetterberg and P. E. M. Siegbahn, *Organometallics*, 1997, **16**, 1933.
40 L. Fan, A. Krzywicki, A. Somogyvari and T. Ziegler, *Inorg. Chem.*, 1996, **35**, 4003.
41 L. Deng, T. K. Woo, L. Cavallo, P. Margl and T. Ziegler, *J. Am. Chem. Soc.*, 1997, **119**, 6177.
42 F. C. Rix, '*Mechanistic studies of palladium(II) mediated carbon-carbon bond formation*', University of North Carolina, Chapel Hill, 1994.
43 A. B. Pangborn, M. A. Giardello, R. H. Grubbs, R. K. Rosea and F. J. Timmers, *Organometallics*, 1996, **15**, 1518.
44 G. Binsch, '*Dynamic Nuclear Magnetic Resonance Spectroscopy*', ed. L. Jackman, and F. A. Cotton, Academic Press, 1975.
45 P. M. Morse, M. D. Spencer, S. R. Wilson and G. S. Girolami, *Organometallics*, 1994, **13**, 1646.
46 J. March, '*Advanced Organic Chemistry*', John Wiley & Sons, 1985.
47 M. Brookhart, B. Grant and A. F. Volpe, Jr., *Organometallics*, 1992, **11**, 3930.
48 J. S. Siegel and F. A. Anet, *J. Org. Chem.*, 1988, **53**, 2629.
49 W. de Graaf, J. Boersma, W. J. J. Smeets, A. L. Spek and G. van Koten, *Organometallics*, 1989, **8**, 2907.
50 R. E. Rülke, J. M. Ernsting, A. L. Spek, C. J. Elsevier, P. W. N. M. Van Leeuwen and K. Vrieze, *Inorg. Chem.*, 1993, **32**, 5769.
51 R. E. Rülke, J. G. P. Delis, A. M. Groot, C. J. Elsevier, P. W. N. M. Van Leeuwen, K. Vrieze, K. Goubitz and H. Schenk, *J. Organomet. Chem.*, 1996, **508**, 109.

